In any event, the effective mass approximation used in the present calculations is most accurate when there is a small number of electrons (or holes), and in that case also, umklapp is of no consequence. But, as these are assumptions compatible with the existence of ferromagnetism, according to the previous arguments, they are therefore quite proper in calculating the properties of a ferromagnet (but not of an antiferromagnet), and are self-consistent.

**ACKNOWLEDGMENTS**

We would like to thank Dr. C. Herring for a very interesting discussion on the subject of magnetism in metals, and Professor T. Nagamiya for discussing his model of antiferromagnetism. We are most grateful to W. Doherty for high-accuracy numerical computations of the solutions to Eq. (28), and to Dr. T. Schultz for many interesting comments on the instability of collective modes in the continuum.

PHYSICAL REVIEW VOLUME 132, NUMBER 6 15 DECEMBER 1963

# Temperature Dependence of the Exchange Stiffness in Ferrimagnets*

TUTO NAKAMURA† AND MICHELINE BLOCH‡
*Department of Physics, University of California, Berkeley, California*
(Received 5 August 1963)

The temperature dependence of magnon frequencies is studied for ferrimagnets. The magnon frequency increases for the acoustical branch and decreases for the optical branch, both in low-temperature regions. Temperature variations obey the $T^{5/2}$ law. In high-temperature regions, both acoustical- and optical-magnon frequencies decrease with increasing temperature. The sign change of the temperature variation of acoustical-magnon frequencies is due to optical-magnon populations which increase with temperature. The sign change occurs at a lower temperature for a magnon with a shorter wavelength. This feature is in accordance with Riste's neutron-scattering experiments performed with magnetites. The second-order shift has proved to be small at low temperatures. In the course of its calculation, we give a simple expression for the matrix element of a magnon interaction. This bears a close relationship to Dyson's dynamical interaction in ferromagnets.

## I. INTRODUCTION

In ferromagnets, the spin-wave frequency (the excitation energy of magnons in units of $\hbar$) decreases with increasing temperature. The decrease is proportional to $T^{5/2}$ at low temperatures. Here $T$ is the temperature in °K. This feature has been given implicitly in the work of Dyson.[1] Oguchi[2] obtained the same result on the basis of the Holstein-Primakoff formalism. Keffer and Loudon[3] gave the expression explicitly for temperature-dependent frequencies on a physical basis. In antiferromagnets[2,3] magnon frequencies also decrease with increasing temperature, where the decrease is proportional to $T^4$ in the absence of anisotropy energies. Recent experiments of the inelastic scattering of neutrons by magnons have made it possible to observe directly the temperature dependence of magnon frequencies.[4,5]

We shall report a notable feature of the temperature dependence of magnon frequencies in ferrimagnets. In ferrimagnets, the magnon spectrum consists of two branches, analogous to the acoustical and optical branches in the vibrational spectrum of diatomic crystals. Long-wavelength magnons in the acoustical branch are similar in their character to that of ferromagnets[6]; the dispersion relation is of the form $\epsilon_\mathbf{k}=Dk^2$. Here $\epsilon_\mathbf{k}$ is an energy of the magnon with a wave vector $\mathbf{k}$. However, the temperature dependence of the *exchange stiffness* $D$ in ferrimagnets is opposite in sign to that in ferromagnets at low temperatures; $D$ increases as $T^{5/2}$. This is caused by the thermal excitation of acoustical magnons. The thermal excitation of optical magnons has the effect of making $D$ decrease more effectively; hence the exchange stiffness decreases sufficiently at high temperature to create a considerable population of optical magnons. Due to competing effects of thermal-acoustical and optical magnons, the temperature dependence of $D$ is rather weak up to a certain high temperature. Magnon frequencies in the optical branch decrease as $T^{5/2}$ due to thermal-acoustical magnons at low temperatures. Thermal-optical magnons work to make optical-magnon frequencies increase. But this effect is weak. Thus optical-magnon frequencies decrease rather rapidly with increasing temperature.

* Supported by the National Science Foundation.

† On leave of absence from the Department of Physics, Osaka University, Osaka, Japan; Kettering Foundation Fellow of Magnetism.

‡ Present address: Centre d'Etudes Nucléaires de Saclay, Gif-sur-Yvette, Seine-et-Oise, France.

[1] F. J. Dyson, Phys. Rev. **102**, 1217 1230 (1956).

[2] T. Oguchi, Phys. Rev. **117**, 117 (1960).

[3] F. Keffer and R. Loudon, J. Appl. Phys. **32**, 2S-7S (1961); see also J. Kanamori and M. Tachiki, J. Phys. Soc. Japan **17**, 1384 (1962).

[4] T. Riste and A. Wanic, J. Phys. Chem. Solids **17**, 318 (1961) (antiferromagnetism); M. Hatherly *et al.* (to be published) (ferromagnetism).

[5] H. Kaplan, Phys. Rev. **86**, 121 (1952); see also P. W. Anderson, lecture given at University of Tokyo, 1954 (unpublished).

[6] For Spin-wave spectrum of magnetites, see T. A. Kaplan, Phys. Rev. **109**, 782 (1958); F. J. Milford and M. L. Glasser, Phys. Letters **2**, 248 (1962).

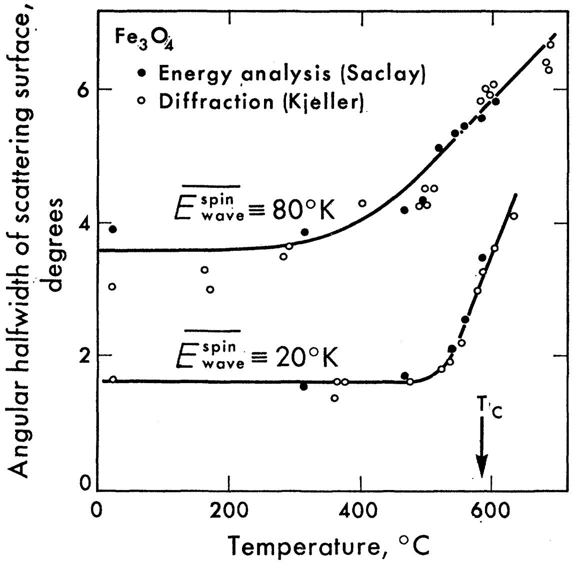


FIG. 1. Temperature variation of the diameter (or angular width) of constant energy surface of magnons (after Riste, Ref. 8).

We also note that different spin-wave modes belonging to the same branch show different temperature behaviors. The increase of the frequency at low temperatures is smaller for acoustical magnons with higher $k$. Thus the net decrease of frequencies to be predicted at high temperatures is more considerable for acoustical magnons with higher $k$.

Our results are based on a two-sublattice model, where the interaction energy is assumed to be

$$H=2J\sum_{\text{n.n.}}\mathbf{S}_j\cdot\mathbf{S}_l. \quad (1)$$

Here $-J$ is the exchange integral with a negative sign, and $\mathbf{S}_j$ and $\mathbf{S}_l$ are nearest-neighbor spins, which belong to different sublattices, "+" and "−," and have different spin quantum numbers, $S_A$ and $S_B$. A sum, $\sum_{\text{n.n.}}$, is extended over all nearest-neighbor pairs. Actual ferrimagnets have complicated structure, as seen in ferrites[6] and garnets.[7] However, the general feature of our results will serve to understand the temperature behaviors of magnon frequencies in actual ferrimagnets.

Our results are consistent with recent observations of the inelastic scattering of neutrons by magnetite.[8] For magnons with an energy of 20°K in units of the Boltzmann constant, the energy increases very slightly or remains almost constant with increasing temperature up to $\sim$750°K, which corresponds to $T/T_c\sim0.9$, where $T_c$ is the Curie point, 848°K for magnetites. Above $T\sim0.9T_c$, the energy decreases rapidly. For magnons with 80°K, a notable decrease of the magnon frequency starts at a lower temperature ($T/T_c\sim0.7$). These features are in accordance with our predictions (see Fig. 1).

We consider first the diagonal term of magnon interactions, which are quartic in the annihilation and creation operators of the deviation of spin from its classical alignment at 0°K. These operators, $a_j$ and $a_l$ and their complex conjugates, are defined by

$$S_j^z=S_A-a_j^*a_j;\quad S_j^-=(2S_A)^{1/2}a_j^*f_j, \quad (2a)$$

and

$$S_l^z=-S_B+b_l^*b_l;\quad S_l^+=(2S_B)^{1/2}b_l^*f_l, \quad (2b)$$

where

$$f_j=(1-a_j^*a_j/2S_A)^{1/2};\quad f_l=(1-b_l^*b_l/2S_B)^{1/2}. \quad (2c)$$

This Holstein-Primakoff formalism reduces to that for antiferromagnets[9] if $S_A=S_B$. As was pointed out by Kasuya,[10] the Holstein-Primakoff formalism works well if the expansions with respect to the reciprocal spin quantum number are carried out properly. The frequency shift due to diagonal terms is of the order $(1/S)^0$, where $S$ is now a mean value of two different spins, $(S_A+S_B)/2$. The shift of the order $1/S$ causes the frequency of acoustical magnons to decrease at low temperatures. This effect was studied also and it proved to be small. As for the frequency shift, the main feature does not change on account of the higher order effect.

In the course of our calculations, we give expressions for the magnon interaction analogous to the dynamical interaction of Dyson,[1] as the result of a decomposition of the relevant matrix element. This decomposition makes evaluations of the second-order shift rather easy.

In Sec. II we give formal developments, together with some aspects in the free-magnon theory. The first-order shift of magnon frequencies is discussed in Sec. III. In Sec. IV, we give expressions for the matrix element of magnon interactions. The second-order shift of magnon frequencies is evaluated in Sec. V. In Sec. VI, we give the detailed temperature behavior of magnon frequencies for both branches, retaining only the first-order shift. There we also take into account the change of magnon populations due to the first-order shift of energies.

## II. FORMAL DEVELOPMENTS

We assume $S_A>S_B$, and put

$$S_A=(1+\alpha)S,\quad S_B=(1-\alpha)S. \quad (3)$$

A parameter $\alpha$ starts with zero and approaches unity with increasing difference in spin quantum numbers. It is equal to $\frac{1}{3}$ for $S_A/S_B=2$, about which we shall give specifically several estimates with particular reference to the CsCl-type structure.

Substituting (2a) and (2b) into (1) and expanding

[7] For Spin-wave spectrum of garnets, see B. Dreyfus, in *Proceedings of the Seventh International Conference on Low-Temperature Physics* (University of Toronto Press, Toronto, 1961), p. 127; M. Tinkham, Phys. Rev. **124**, 311 (1961).

[8] T. Riste, J. Phys. Soc. Japan **17**, Suppl. B-III (1962).

[9] R. Kubo, Phys. Rev. **87**, 568 (1952).

[10] T. Kasuya, Busseiron Kenkyu **92**, 14 (1956).

$f_j$ and $f_l$ defined by (2c) in a power series of $1/S_A$ and $1/S_B$ ,we have a series

$$H=H_0+H_1+H_2+\cdots, \tag{4}$$

apart from the leading constant term which equals the classical energy to be obtained in a complete antiparallel alignment of spins. Here $H_0$, $H_1$, and $H_2$ are terms of the order $S^1$, $S^0$, and $S^{-1}$, respectively. We introduce the Fourier transforms of $a_j$ and $a_l$:

$$\begin{aligned} a_{\mathbf{k}}&=N^{-1/2}\sum_j a_j[\exp(-i\mathbf{k}\cdot\mathbf{R}_j)];\\ b_{\mathbf{k}}&=N^{-1/2}\sum_l b_l[\exp(i\mathbf{k}\cdot\mathbf{R}_l)], \end{aligned} \tag{5}$$

where $\mathbf{R}_j$ and $\mathbf{R}_l$ are the position vectors of lattice points belonging to "+" and "−" sublattices, respectively, and $N$ is the number of spins belonging to a sublattice. Then $H_0$, $H_1$, and $H_2$ are written

$$H_0=2J\sum_{\mathbf{k}}[\gamma_0(S_Ba_{\mathbf{k}}^*a_{\mathbf{k}}+S_Ab_{\mathbf{k}}^*b_{\mathbf{k}})+(S_AS_B)^{1/2}\gamma_{\mathbf{k}}(a_{\mathbf{k}}b_{\mathbf{k}}+a_{\mathbf{k}}^*b_{\mathbf{k}}^*)]; \tag{6}$$

$$\begin{aligned} H_1=-(2N)^{-1}J(S_AS_B)^{-1/2}\sum_{\mathbf{k}_1\ldots\mathbf{k}_4}[&S_B\gamma_{\mathbf{k}1}b_{\mathbf{k}1}a_{\mathbf{k}2}^*a_{\mathbf{k}3}a_{\mathbf{k}4}\\ &+S_A\gamma_{\mathbf{k}1}a_{\mathbf{k}1}b_{\mathbf{k}2}^*b_{\mathbf{k}3}b_{\mathbf{k}4}\\ &+2(S_AS_B)^{1/2}\gamma_{\mathbf{k}1-\mathbf{k}3}a_{\mathbf{k}1}^*a_{\mathbf{k}3}b_{\mathbf{k}4}^*b_{\mathbf{k}2}]\\ &\times\delta(\mathbf{k}_1+\mathbf{k}_2-\mathbf{k}_3-\mathbf{k}_4)+\text{c.c.}; \end{aligned} \tag{7}$$

$$\begin{aligned} H_2=-(4N)^{-2}J(S_AS_B)^{-3/2}&\\ \times\sum_{\mathbf{k}_1\ldots\mathbf{k}_6}\{&S_A^2\gamma_{\mathbf{k}1}a_{\mathbf{k}1}^*b_{\mathbf{k}4}^*b_{\mathbf{k}5}^*b_{\mathbf{k}2}b_{\mathbf{k}6}^*b_{\mathbf{k}3}\\ &-2S_AS_B\gamma_{\mathbf{k}1+\mathbf{k}2-\mathbf{k}4}a_{\mathbf{k}1}^*a_{\mathbf{k}2}^*a_{\mathbf{k}4}b_{\mathbf{k}5}^*b_{\mathbf{k}6}^*b_{\mathbf{k}3}\\ &+S_B^2\gamma_{\mathbf{k}6}a_{\mathbf{k}1}^*a_{\mathbf{k}2}^*a_{\mathbf{k}4}a_{\mathbf{k}3}^*a_{\mathbf{k}5}b_{\mathbf{k}6}^*\}\\ &\times\delta(\mathbf{k}_1+\mathbf{k}_2+\mathbf{k}_3-\mathbf{k}_4-\mathbf{k}_5-\mathbf{k}_6)+\text{c.c.} \end{aligned} \tag{8}$$

Here $\gamma_0$ is the number of nearest neighbors, and

$$\gamma_{\mathbf{k}}=\sum_{\boldsymbol{\delta}}\exp(i\mathbf{k}\cdot\boldsymbol{\delta}), \tag{9}$$

in which $\boldsymbol{\delta}$ is a vector to nearest neighbors.

The Hamiltonian $H_0$, which describes free magnons, gives the magnon energies

$$\begin{aligned} \epsilon_{\mathbf{k}\alpha}^0&=2\gamma_0JS(f_{\mathbf{k}}-\alpha);\\ \epsilon_{\mathbf{k}\beta}^0&=2\gamma_0JS(f_{\mathbf{k}}+\alpha), \end{aligned} \tag{10}$$

where

$$f_{\mathbf{k}}=[1-(1-\alpha^2)(\gamma_{\mathbf{k}}/\gamma_0)^2]^{1/2}. \tag{11}$$

The excitation energies, $\epsilon_{\mathbf{k}\alpha}^0$ and $\epsilon_{\mathbf{k}\beta}^0$, are associated with the spin-wave modes $\alpha_{\mathbf{k}}$ and $\beta_{\mathbf{k}}$ respectively, which are given by

$$\begin{aligned} a_{\mathbf{k}}&=u_{\mathbf{k}}\alpha_{\mathbf{k}}-v_{\mathbf{k}}\beta_{\mathbf{k}}^*;\\ b_{\mathbf{k}}&=-v_{\mathbf{k}}\alpha_{\mathbf{k}}^*+u_{\mathbf{k}}\beta_{\mathbf{k}}. \end{aligned} \tag{12}$$

Here $u_{\mathbf{k}}$ and $v_{\mathbf{k}}$ are defined by

$$\begin{aligned} u_{\mathbf{k}}^2-v_{\mathbf{k}}^2&=1;\\ 2u_{\mathbf{k}}v_{\mathbf{k}}&=(1-\alpha^2)^{1/2}(\gamma_{\mathbf{k}}/\gamma_0)/f_{\mathbf{k}}. \end{aligned} \tag{13}$$

The magnons associated with $\alpha_{\mathbf{k}}$ and $\beta_{\mathbf{k}}$ will hereafter be called $\alpha$ and $\beta$ magnons, respectively. As seen in (11), $f_{\mathbf{k}}$ starts with $\alpha$ and approaches unity as $k$ increases from zero. Thus the bottom of the band is zero for $\alpha$ magnons and $4\gamma_0JS\alpha$ for $\beta$ magnons. The respective modes are responsible for the ferromagnetic and exchange resonances. The top of the $\alpha$ band is $2\gamma_0JS(1-\alpha)$, which is the energy needed to reverse the direction of a single $B$ spin. The top of the $\beta$ band is $2\gamma_0JS(1+\alpha)$, which is the energy needed to reverse the direction of a single $A$ spin. The relative position of bands is shown schematically in Fig. 2.

If we use a long-wavelength approximation

$$\gamma_{\mathbf{k}}\cong\gamma_0-(ka)^2, \tag{14}$$

(11) becomes

$$f_{\mathbf{k}}\cong\alpha+(1/\gamma_0)[(1-\alpha^2)/\alpha](ka)^2, \tag{15}$$

where $a$ is the lattice constant. Then (10) is written

$$\begin{aligned} \epsilon_{\mathbf{k}\alpha}^0&\cong2JS(1-\alpha^2)/\alpha(ka)^2;\\ \epsilon_{\mathbf{k}\beta}^0&\cong4\gamma_0JS\alpha+2JS(1-\alpha^2)/\alpha(ka)^2, \end{aligned} \tag{16}$$

in a long-wavelength approximation.

The zero-point energy becomes

$$-2N\gamma_0JS(1-N^{-1}\sum_{\mathbf{k}}f_{\mathbf{k}}). \tag{17}$$

The last factor is estimated to be 0.063 for a CsCl-type structure with $\alpha=\frac{1}{3}$ (see Table III, Sec. V). This estimate is compared with 0.073 for the same lattice in the antiferromagnetic case ($\alpha=0$).

Average magnon energies for $\alpha$ and $\beta$ bands are

$$N\epsilon_\alpha^0=\sum_{\mathbf{k}}\bar{n}_{\mathbf{k}\alpha}\epsilon_{\mathbf{k}\alpha}^0,\quad N\epsilon_\beta^0=\sum_{\mathbf{k}}\bar{n}_{\mathbf{k}\beta}\epsilon_{\mathbf{k}\beta}^0, \tag{18}$$

where $\bar{n}_{\mathbf{k}\alpha}$ and $\bar{n}_{\mathbf{k}\beta}$ are thermal populations. In the long-wavelength approximation, we have

$$\epsilon_\alpha^0\cong BT^{5/2}; \tag{19}$$

$$B=\tfrac{3}{2}\zeta(\tfrac{5}{2})\left\{\frac{\alpha}{1-\alpha^2}\frac{k_B}{8\pi JS}\right\}^{3/2}k_B, \tag{19a}$$

in which $(\zeta\frac{5}{2})=1.341$ and $k_B$ is the Boltzmann constant. Similarly, we evaluate $\epsilon_\beta^0$ as

$$\epsilon_\beta^0\cong\left\{\frac{\alpha}{1-\alpha^2}\frac{k_BT}{8\pi JS}\right\}^{3/2}\epsilon_{0\beta}^0\exp\left(-\frac{\epsilon_{0\beta}^0}{k_BT}\right), \tag{20}$$

where $\epsilon_{0\beta}^0$ is the energy at the bottom of the $\beta$ band.

## III. FIRST-ORDER SHIFT

The first-order shift of magnon energies comes from the diagonal term of $H_1$ given by (7). This diagonal term is included in the following expression

$$\begin{aligned} -N^{-1}J(S_AS_B)^{-1/2}\sum_{\mathbf{k},\mathbf{k}'}[&(S_B\gamma_{\mathbf{k}}a_{\mathbf{k}'}^*a_{\mathbf{k}'}a_{\mathbf{k}}b_{\mathbf{k}}\\ &+S_A\gamma_{\mathbf{k}}a_{\mathbf{k}}b_{\mathbf{k}'}^*b_{\mathbf{k}}b_{\mathbf{k}'})+(S_AS_B)^{1/2}(\gamma_0a_{\mathbf{k}}^*a_{\mathbf{k}}b_{\mathbf{k}'}^*b_{\mathbf{k}'}\\ &+\gamma_{\mathbf{k}-\mathbf{k}'}a_{\mathbf{k}}^*b_{\mathbf{k}}^*a_{\mathbf{k}'}b_{\mathbf{k}'})]+\text{c.c.} \end{aligned} \tag{21}$$

On substituting (12) into (21), we have three types of diagonal terms in $\alpha_{\mathbf{k}}$ and $\beta_{\mathbf{k}}$; the term independent of

$n_{k\alpha}$ and $n_{k\beta}$, and the linear and quadratic terms in $n_{k\alpha}$ and $n_{k\beta}$.

The term linear in $n_{k\alpha}$ and $n_{k\beta}$ is written

$$\Delta E_1^{(1)} = \sum_{\mathbf{k}} [\Gamma_\alpha(\mathbf{k}) n_{k\alpha} + \Gamma_\beta(\mathbf{k}) n_{k\beta}], \qquad (22)$$

where

$$\begin{aligned}\Gamma_\alpha(\mathbf{k}) = -\gamma_0 J (f_k^{-1}[1-(\gamma_k/\gamma_0)^2]N^{-1} \\ \times \sum_{k'} \{f_{k'}^{-1}[1-(\gamma_{k'}/\gamma_0)^2]-1\} \\ +[1-\alpha f_k^{-1}(\gamma_k/\gamma_0)^2]N^{-1} \\ \times \sum_{k'} \alpha f_{k'}^{-1}(\gamma_{k'}/\gamma_0)^2), \qquad (23)\end{aligned}$$

$$\Gamma_\beta(\mathbf{k}) = \Gamma_\alpha(\mathbf{k}) + 2\gamma_0 J N^{-1} \sum_{k'} \alpha f_{k'}^{-1}(\gamma_{k'}/\gamma_0)^2.$$

Here we used (13) also. The frequency shifts at 0°K are given by $\Gamma_\alpha(\mathbf{k})$ and $\Gamma_\beta(\mathbf{k})$ for $\alpha$ and $\beta$ magnons, respectively. The shift $\Gamma_\alpha(\mathbf{k})$ vanishes at $k=0$ and becomes

$$\Gamma_\alpha(\mathbf{k}) \cong -J\alpha^{-1}(ka)^2[N^{-1}\sum_{k'}(f_{k'}^{-1}+f_{k'}-2)]$$

in long-wavelength regions. With an estimate of the last factor, 0.0247, for our particular case, the relative shift, $\Gamma_\alpha(\mathbf{k})/\epsilon_{k\alpha}^0$, is $-0.0139/S$. The shift $\Gamma_\alpha(\mathbf{k})$ is negative for small $k$, but changes its sign for large $k$; $\Gamma_\alpha(\mathbf{k})$ at the top of the band is $+0.026(\gamma_0 J)$ with a relative shift $+0.020/S$. On the other hand, the shift $\Gamma_\beta(\mathbf{k})/\epsilon_{k\beta}^0$, is estimated to be $+0.086/S$ at the bottom and $+0.052/S$ at the top of the band.

From the above analysis, we observe that the temperature-independent frequency shift is smaller for the $\alpha$ mode than for the $\beta$ mode and that the largest relative shift occurs at the exchange-resonance mode. This feature will be preserved also in the temperature-dependent frequency shift.

The diagonal term quadratic in $n_{k\alpha}$ and $n_{k\beta}$ gives rise to the temperature-dependent frequency shift, and is written

$$\begin{aligned}\Delta E_1^{(2)} = \sum_{k,k'} [\tfrac{1}{2}\Gamma_{\alpha\alpha}(\mathbf{k},\mathbf{k}') n_{k\alpha} n_{k'\alpha} + \Gamma_{\alpha\beta}(\mathbf{k},\mathbf{k}') n_{k\alpha} n_{k'\beta} \\ + \tfrac{1}{2}\Gamma_{\beta\beta}(\mathbf{k},\mathbf{k}') n_{k\beta} n_{k'\beta}] \qquad (25)\end{aligned}$$

from (21), using (13), where

$$\begin{aligned}\Gamma_{\alpha\alpha}(\mathbf{k},\mathbf{k}') = N^{-1}\gamma_0 J \Bigg\{ \left[1-\frac{\alpha}{f_k}\left(\frac{\gamma_k}{\gamma_0}\right)^2\right]\left[1-\frac{\alpha}{f_{k'}}\left(\frac{\gamma_{k'}}{\gamma_0}\right)^2\right] \\ -\frac{1}{f_k f_{k'}}\left[1-\left(\frac{\gamma_k}{\gamma_0}\right)^2\right]\left[1-\left(\frac{\gamma_{k'}}{\gamma_0}\right)^2\right] \\ -\frac{1-\alpha^2}{f_k f_{k'}}\left(\frac{\gamma_k}{\gamma_0}\cdot\frac{\gamma_{k'}}{\gamma_0}\right)\left(\frac{\gamma_{k-k'}}{\gamma_0}-\frac{\gamma_k\gamma_{k'}}{\gamma_0^2}\right)\Bigg\}; \qquad (26)\end{aligned}$$

$$\begin{aligned}\Gamma_{\alpha\beta}(\mathbf{k},\mathbf{k}') = \Gamma_{\alpha\alpha}(\mathbf{k},\mathbf{k}') - 2N^{-1}\gamma_0 J \\ + 2N^{-1}\gamma_0 J \alpha f_k^{-1}(\gamma_k/\gamma_0)^2;\end{aligned}$$

$$\begin{aligned}\Gamma_{\beta\beta}(\mathbf{k},\mathbf{k}') = \Gamma_{\alpha\alpha}(\mathbf{k},\mathbf{k}') + 2N^{-1}\gamma_0 J\alpha\{f_k^{-1}(\gamma_k/\gamma_0)^2 \\ + f_{k'}^{-1}(\gamma_{k'}/\gamma_0)^2\}.\end{aligned}$$

Here $\Gamma_{\alpha\alpha}(\mathbf{k},\mathbf{k}')$ and $\Gamma_{\beta\beta}(\mathbf{k},\mathbf{k}')$ are symmetrical with $\mathbf{k}$ and $\mathbf{k}'$, but $\Gamma_{\alpha\beta}(\mathbf{k},\mathbf{k}') = \Gamma_{\beta\alpha}(\mathbf{k}',\mathbf{k})$.

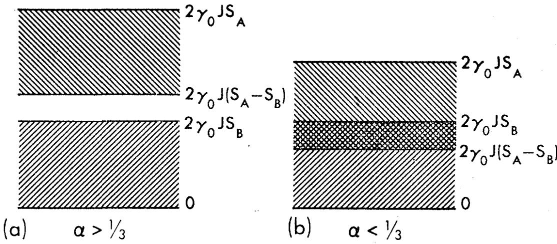


FIG. 2. Magnon energy bands for ferrimagnets.

The temperature-dependent shifts, $\Delta\epsilon_{k\alpha}$ and $\Delta\epsilon_{k\beta}$, are given now by

$$\begin{aligned}\Delta\epsilon_{k\alpha} = \sum_{k'} \Gamma_{\alpha\alpha}(\mathbf{k},\mathbf{k}')\bar{n}_{k'\alpha} + \sum_{k'} \Gamma_{\alpha\beta}(\mathbf{k},\mathbf{k}')\bar{n}_{k'\beta}; \\ \Delta\epsilon_{k\beta} = \sum_{k'} \Gamma_{\beta\alpha}(\mathbf{k},\mathbf{k}')\bar{n}_{k'\alpha} + \sum_{k'} \Gamma_{\beta\beta}(\mathbf{k},\mathbf{k}')\bar{n}_{k'\beta}.\end{aligned} \qquad (27)$$

This is easily shown by forming the equations of motion of $\alpha_k$ and $\beta_k$, including (25), where the torques dependent on the occupation numbers are replaced by their thermal average. Due to the cubic symmetry of $\bar{n}_{k'\alpha}$ with respect to $\mathbf{k}'$, we have

$$\sum_{k'} \gamma_{k'}\gamma_{k-k'}\bar{n}_{k'\alpha} = (\gamma_k/\gamma_0)\sum_{k'} \gamma_{k'}^2 \bar{n}_{k'}\alpha. \qquad (28)$$

Hence the last term in braces of (26) does not contribute to (27), but it does contribute to the fluctuation effects. By assuming a "random-phase approximation," $\Gamma_{\alpha\alpha}(\mathbf{k},\mathbf{k}')$, etc., can be written in simple forms, using (11),

$$\begin{aligned}\Gamma_{\alpha\alpha}(\mathbf{k},\mathbf{k}') = M(f_k-\alpha)(f_{k'}-\alpha)[(f_k f_{k'})^{-1}-1]; \\ \Gamma_{\alpha\beta}(\mathbf{k},\mathbf{k}') = -M(f_k-\alpha)(f_{k'}+\alpha)[(f_k f_{k'})^{-1}+1]; \qquad (29) \\ \Gamma_{\beta\beta}(\mathbf{k},\mathbf{k}') = M(f_k+\alpha)(f_{k'}+\alpha)[(f_k f_{k'})^{-1}-1],\end{aligned}$$

where

$$M = N^{-1}(\gamma_0 J)/(1-\alpha^2). \qquad (29a)$$

The last factors in (29) are always positive. Hence the frequency shift due to thermal $\alpha$ magnons is positive for an $\alpha$ magnon and negative for a $\beta$ magnon, whereas the shift due to thermal $\beta$ magnons is negative for an $\alpha$ magnon and positive for a $\beta$ magnon. The effect of $\Gamma_{\alpha\beta}$ on the shift is stronger than that of $\Gamma_{\alpha\alpha}$ and $\Gamma_{\beta\beta}$.

In low-temperature regions, we have approximately

$$\frac{\Delta\epsilon_{k\alpha}}{\epsilon_{k\alpha}^0} \cong \sum_{k'} \Gamma_{\alpha\alpha}(\mathbf{k},\mathbf{k}')\bar{n}_{k'\alpha}/\epsilon_{k\alpha}^0 \cong \frac{(\alpha f_k)^{-1}}{4\gamma_0 J S^2}\cdot\frac{1-\alpha f_k}{1-\alpha^2}\epsilon_\alpha^0. \qquad (30)$$

Thus the relative shift of the $\alpha$-magnon frequency increases as $T^{5/2}$ with increasing temperature [cf. (19)]. The increase is dependent on the wavevector associated with magnons; the temperature coefficient of the relative shift for magnons near the bottom is $(1+\alpha)/\alpha$ times larger than that for magnons at the top of the band. For $\beta$ magnons, the shift becomes

$$\frac{\Delta\epsilon_{k\beta}}{\epsilon_{k\beta}^0} \cong -\frac{(\alpha f_k)^{-1}}{4\gamma_0 J S^2}\cdot\frac{1+\alpha f_k}{1-\alpha^2}\epsilon_\alpha^0, \qquad (31)$$

with a negative temperature coefficient. The magnitude of the temperature coefficient at the bottom is $\alpha^{-1}(1+\alpha^2)/(1+\alpha)$ times larger than that at the top of the band.

It may be interesting to compare the temperature-dependent shift in ferrimagnets with that in antiferromagnets. The latter is predicted by considering the case with the limit $\alpha=0$. In this limit, $\Gamma_{\alpha\alpha}$, $\Gamma_{\alpha\beta}$, and $\Gamma_{\beta\beta}$ are given, respectively, by

$$1-f_{\mathbf{k}}f_{\mathbf{k}'}, \quad -(1+f_{\mathbf{k}}f_{\mathbf{k}'}), \quad 1-f_{\mathbf{k}}f_{\mathbf{k}'}, \tag{32}$$

apart from a proportional constant, where $f_{\mathbf{k}}$ is now proportional to the frequency associated with a wave-vector $\mathbf{k}$. Because $\epsilon_{\mathbf{k}\alpha}{}^0=\epsilon_{\mathbf{k}\beta}{}^0$ in the absence of the magnetic field, we have $\bar{n}_{\mathbf{k}\alpha}=\bar{n}_{\mathbf{k}\beta}$ in antiferromagnets. Hence the contributions of the respective first terms in (32), 1, $-1$, and 1, to $\Delta\epsilon_{\mathbf{k}\alpha}$ and $\Delta\epsilon_{\mathbf{k}\beta}$ are canceled by each other. The net result is a decrease in frequency with the same relative shift for all modes.

The feature just mentioned disappears in ferrimagnets due to a frequency difference between two modes with the same $\mathbf{k}$, giving rise to a frequency increase of low-lying magnons at low temperatures. However, as will be seen in Sec. VI, the increase of $\beta$-magnon populations makes the shift of the $\alpha$ magnon change its sign; the $\alpha$-magnon frequency starts to go down at a certain high temperature.

We finally give the population-independent term of (21):

$$\Delta E_1{}^{(0)}=\tfrac{1}{2}N\gamma_0 J\left\{\left[N^{-1}\sum_{\mathbf{k}}\left(1+\frac{\alpha^2}{1-\alpha^2}f_{\mathbf{k}}{}^{-1}-\frac{1}{1-\alpha^2}f_{\mathbf{k}}\right)\right]^2 -\frac{\alpha^2}{(1-\alpha^2)^2}\left[N^{-1}\sum_{\mathbf{k}}(f_{\mathbf{k}}{}^{-1}-f_{\mathbf{k}})\right]^2\right\}, \tag{33}$$

which is a correction to the zero-point energy of the system. An estimate of the last factor $\{\cdots\}$ is 0.0035 for our particular case. This estimate is compared with the corresponding one, 0.0053, in the case with limit $\alpha=0$.

## IV. MATRIX ELEMENTS OF THE MAGNON INTERACTION

In order to see the second-order energy shift and the exchange relaxation of magnons, we need to deal with nondiagonal components of the quartic term $H_1$ given by (7). These components seem to have a complicated structure, as is seen on substituting (12) into (7). However, the matrix element should vanish for the real process of transitions if the $\mathbf{k}=0$ mode of the acoustical branch participates in the transition, because that mode only represents a uniform rotation of the spin system. The real process comes from the matrix elements satisfying energy conservation. Thus we decompose a matrix element of $H_1$ into two parts: the part that vanishes in the real process and the remaining part. The first part has a factor of the energy difference between the initial and final states for a relevant transition. The second part vanishes for transitions where the mode $\alpha_0$ participates in the initial (or final) state.

The present decomposition bears a close relationship to Dyson's classification of the magnon interaction. There is classification into dynamical and kinematical parts. We first show that in ferromagnets the second part of matrix elements decomposed just gives the dynamical interaction of Dyson. Assuming the Hamiltonian in this case to be given by (1), with negative sign and $S_A=S_B\equiv S$, we write quartic terms of the Hamiltonian in the following:

$$(H_1)_{\text{ferro}}=4^{-1}\sum_{\mathbf{k}_1\ldots\mathbf{k}_4}V(\mathbf{k}_1,\mathbf{k}_2;\mathbf{k}_3,\mathbf{k}_4)a_{\mathbf{k}1}{}^*a_{\mathbf{k}2}{}^*a_{\mathbf{k}3}a_{\mathbf{k}4}\times\delta(\mathbf{k}_1+\mathbf{k}_2-\mathbf{k}_3-\mathbf{k}_4), \tag{34}$$

where $a_{\mathbf{k}}$ and $a_{\mathbf{k}}{}^*$ are defined by (2a), and

$$V(\mathbf{k}_1,\mathbf{k}_2;\mathbf{k}_3,\mathbf{k}_4)=N^{-1}J(\gamma_{\mathbf{k}1}+\gamma_{\mathbf{k}2}+\gamma_{\mathbf{k}3}+\gamma_{\mathbf{k}4}-2\gamma_{\mathbf{k}1-\mathbf{k}4}-2\gamma_{\mathbf{k}1-\mathbf{k}3}). \tag{35}$$

Equation (35) is rewritten

$$V(\mathbf{k}_1,\mathbf{k}_2;\mathbf{k}_3,\mathbf{k}_4)=V_1(\mathbf{k}_1,\mathbf{k}_2;\mathbf{k}_3,\mathbf{k}_4)+V_2(\mathbf{k}_1,\mathbf{k}_2;\mathbf{k}_3,\mathbf{k}_4). \tag{36}$$

Here

$$V_1=N^{-1}J(\gamma_{\mathbf{k}3}+\gamma_{\mathbf{k}4}-\gamma_{\mathbf{k}1}-\gamma_{\mathbf{k}2}); \tag{37a}$$

$$V_2=2N^{-1}J\sum_{\delta}\exp(i\mathbf{q}\cdot\boldsymbol{\delta})[\exp(i\mathbf{k}\cdot\boldsymbol{\delta})-1]\times[1-\exp(-i\mathbf{k}'\cdot\boldsymbol{\delta})], \tag{37b}$$

where $\mathbf{q}=\mathbf{k}_1-\mathbf{k}_3=\mathbf{k}_4-\mathbf{k}_2$, $\mathbf{k}_3\equiv\mathbf{k}$, and $\mathbf{k}_4\equiv\mathbf{k}'$. Remembering that the magnon energy is given now by $\epsilon_{\mathbf{k}}{}^0=2JS(\gamma_0-\gamma_{\mathbf{k}})$, we write $V_1$ as

$$V_1=(2NS)^{-1}(\epsilon_{\mathbf{k}1}{}^0+\epsilon_{\mathbf{k}2}{}^0-\epsilon_{\mathbf{k}3}{}^0-\epsilon_{\mathbf{k}4}{}^0). \tag{38}$$

As is apparent in (38), $V_1$ vanishes identically for the real process. On the other hand, $V_2$ gives the dynamical interaction of Dyson. It may be noted that each of the $V_1$ and $V_2$ is no longer Hermitian except for the real process, although $V=V_1+V_2$ has a Hermitian property.

The decomposition just given for the case of a ferromagnet may look more or less self-evident. However, we described it in detail because the procedure for ferrimagnets is completely parallel, although the matrix elements become more complicated.

Several different processes are included in $H_1$ which are given in Fig. 2 where the solid lines represent the $\alpha$ magnon and the broken lines the $\beta$ magnon. Processes II and VI are generated by process I if we remember that there exists a process to be derived from a figure with the replacement of a solid line on the left side by a broken line on the right side of the figure and vice versa. In the derived figure, the direction of $\mathbf{q}$ should be changed. There are also processes inverse to those given in Fig. 3.

A matrix element $V(n)$ for a process $n$ is decomposed into two parts

$$V(n)=V_1(n)+V_2(n). \tag{39}$$

TABLE I. Expressions for $V_1(n)$. Here $n$ designates a process given in Fig. 2, and we put

$$V_1(n)=(2N)^{-1}(X_n/S_A-Y_n/S_B)\varphi_n,\quad u_{\mathbf{k}}=[(1+f_{\mathbf{k}})/(2f_{\mathbf{k}})]^{1/2},\quad v_{\mathbf{k}}=[(1-f_{\mathbf{k}})/(2f_{\mathbf{k}})]^{1/2}\,\mathrm{sgn}\gamma_{\mathbf{k}},$$

in which $\mathrm{sgn}\gamma_{\mathbf{k}}$ is $+1$ for $\gamma_{\mathbf{k}}>0$ and $-1$ for $\gamma_{\mathbf{k}}<0$.

| Process ($n$) | $X_n$ | $Y_n$ | $\varphi_n$ |
|---|---|---|---|
| I | $u_{\mathbf{k}}u_{\mathbf{k}'}u_{\mathbf{k}+\mathbf{q}}u_{\mathbf{k}'-\mathbf{q}}$ | $v_{\mathbf{k}}v_{\mathbf{k}'}v_{\mathbf{k}+\mathbf{q}}v_{\mathbf{k}'-\mathbf{q}}$ | $\epsilon_{\mathbf{k}+\mathbf{q}\alpha}{}^0+\epsilon_{\mathbf{k}'-\mathbf{q}\alpha}{}^0-\epsilon_{\mathbf{k}\alpha}{}^0-\epsilon_{\mathbf{k}'\alpha}{}^0$ |
| II | $u_{\mathbf{k}}v_{\mathbf{k}'}u_{\mathbf{k}+\mathbf{q}}v_{\mathbf{k}'+\mathbf{q}}$ | $v_{\mathbf{k}}u_{\mathbf{k}'}v_{\mathbf{k}+\mathbf{q}}u_{\mathbf{k}'+\mathbf{q}}$ | $\epsilon_{\mathbf{k}+\mathbf{q}\alpha}{}^0+\epsilon_{\mathbf{k}'+\mathbf{q}\beta}{}^0-\epsilon_{\mathbf{k}\alpha}{}^0-\epsilon_{\mathbf{k}'\beta}{}^0$ |
| III | $v_{\mathbf{k}}v_{\mathbf{k}'}v_{\mathbf{k}+\mathbf{q}}v_{\mathbf{k}'-\mathbf{q}}$ | $u_{\mathbf{k}}u_{\mathbf{k}'}u_{\mathbf{k}+\mathbf{q}}u_{\mathbf{k}'-\mathbf{q}}$ | $-\epsilon_{\mathbf{k}+\mathbf{q}\beta}{}^0-\epsilon_{\mathbf{k}'-\mathbf{q}\beta}{}^0+\epsilon_{\mathbf{k}\beta}{}^0+\epsilon_{\mathbf{k}'\beta}{}^0$ |
| IV | $u_{\mathbf{k}}u_{\mathbf{k}'}u_{\mathbf{k}+\mathbf{q}}v_{\mathbf{k}'+\mathbf{q}}$ | $v_{\mathbf{k}}v_{\mathbf{k}'}v_{\mathbf{k}+\mathbf{q}}u_{\mathbf{k}'+\mathbf{q}}$ | $-\epsilon_{\mathbf{k}+\mathbf{q}\alpha}{}^0-\epsilon_{\mathbf{k}'+\mathbf{q}\beta}{}^0-\epsilon_{\mathbf{k}'\alpha}{}^0+\epsilon_{\mathbf{k}\alpha}{}^0$ |
| V | $v_{\mathbf{k}}v_{\mathbf{k}'}v_{\mathbf{k}+\mathbf{q}}u_{\mathbf{k}'+\mathbf{q}}$ | $u_{\mathbf{k}}u_{\mathbf{k}'}u_{\mathbf{k}+\mathbf{q}}v_{\mathbf{k}'+\mathbf{q}}$ | $\epsilon_{\mathbf{k}+\mathbf{q}\beta}{}^0+\epsilon_{\mathbf{k}'+\mathbf{q}\alpha}{}^0+\epsilon_{\mathbf{k}'\beta}{}^0-\epsilon_{\mathbf{k}\beta}{}^0$ |
| VI | $u_{\mathbf{k}}u_{\mathbf{k}'}v_{\mathbf{k}+\mathbf{q}}v_{\mathbf{k}'-\mathbf{q}}$ | $v_{\mathbf{k}}v_{\mathbf{k}'}u_{\mathbf{k}+\mathbf{q}}u_{\mathbf{k}'-\mathbf{q}}$ | $-(\epsilon_{\mathbf{k}+\mathbf{q}\beta}{}^0+\epsilon_{\mathbf{k}'-\mathbf{q}\beta}{}^0+\epsilon_{\mathbf{k}\alpha}{}^0+\epsilon_{\mathbf{k}'\alpha}{}^0)$ |

Here $V_1(n)$ is a part vanishing in the real process, or a part with a factor of the energy difference between the initial and final states of the transition, and $V_2(n)$ is an expression analogous to the dynamical interaction of Dyson. These two components are given in Tables I and II respectively. One of the expressions is derived in Appendix A. If we replace $V_1(n)$ by $-V_1(n)$, we have another expression for the "dynamical part,"

$$V(n)=-V_1(n)+\tilde{V}_2(n). \tag{40}$$

For process IV, $\tilde{V}_2$ becomes

$$\tilde{V}_2(\mathrm{IV})=-(2/N)J(1-\alpha^2)^{-1/2}\sum_\delta(\xi v_{\mathbf{k}'}e_{\mathbf{k}'}-\eta u_{\mathbf{k}'})\times(\xi v_{\mathbf{k}+\mathbf{q}}e_{\mathbf{k}+\mathbf{q}}-\eta u_{\mathbf{k}+\mathbf{q}})(u_{\mathbf{k}}u_{\mathbf{k}'+\mathbf{q}}e_{-\mathbf{k}'-\mathbf{q}}+v_{\mathbf{k}}v_{\mathbf{k}'+\mathbf{q}}e_{-\mathbf{k}}), \tag{41}$$

with the same convention as given in Table II. The corresponding expression for process $V$ is derived from (41) by interchanging $u$ and $v$. We omit the expression for $\tilde{V}_2(\mathrm{VI})$ for the sake of brevity.

As is apparent in Table II $V_2$ vanishes for transitions with the participation of the uniform mode $\alpha_0$ in the initial state, but not in the final state. This is true also for $\tilde{V}_2$, if we interchange literally the initial and final states. This non-Hermitian property of $V_2$ disappears for the real transition. In this particular transition, the second part of $V$ vanishes with the participation of the uniform mode in any one of the initial and final states.

## V. SECOND-ORDER SHIFT

In ferromagnets, the second-order shift of magnon energies has the same sign as the first-order shift in long-wavelength regions. However, this is not the case in ferrimagnets. As seen in Sec. III, the first-order shift for low-lying magnons is positive at low temperatures. This effect may be weakened by the second-order shift, which we shall proceed to investigate.

The second-order shift is troublesome to evaluate in ferrimagnets; hence we shall limit our calculations to long-wavelength $\alpha$ magnons at low temperatures. This is obtained from an energy correction,

$$\tfrac{1}{2}\sum_{\mathbf{k},\mathbf{k}'}\Gamma_{\alpha\alpha}{}^{(2)}(\mathbf{k},\mathbf{k}')n_{\mathbf{k}\alpha}n_{\mathbf{k}'\alpha'}, \tag{42}$$

where $\Gamma_{\alpha\alpha}{}^{(2)}(\mathbf{k},\mathbf{k}')$ is of the order $1/S$. We denote $\Gamma_{\alpha\alpha}(\mathbf{k},\mathbf{k}')$, which is given by (26) or (29), by $\Gamma_{\alpha\alpha}{}^{(1)}(\mathbf{k},\mathbf{k}')$. Energies quadratic in $n_{\mathbf{k}\alpha}$ are expressed in terms of $\Gamma_{\alpha\alpha}(\mathbf{k},\mathbf{k}')$.

$$\Gamma_{\alpha\alpha}(\mathbf{k},\mathbf{k}')=\Gamma_{\alpha\alpha}{}^{(1)}(\mathbf{k},\mathbf{k}')+\Gamma_{\alpha\alpha}{}^{(2)}(\mathbf{k},\mathbf{k}')+\cdots. \tag{43}$$

This is a power series in $1/S$. The initial term becomes

$$\Gamma_{\alpha\alpha}{}^{(1)}(\mathbf{k},\mathbf{k}')\cong\frac{J}{N\gamma_0}\left(\frac{1-\alpha^2}{\alpha^2}\right)^2(ka)^2(k'a)^2 \tag{44}$$

in a long-wavelength approximation.

TABLE II. Expressions for $V_2(n)$. Here we put

$$V_2(n)=(2/N)(1-\alpha^2)^{-1/2}J\,\Sigma_\delta g_1g_2h,$$

$\exp(i\mathbf{k}\cdot\boldsymbol{\delta})=e_{\mathbf{k}}$ and $(1+\alpha)^{1/2}=\xi$, $(1-\alpha)^{1/2}=\eta$. Otherwise we use the same notations as given in Table I.

| Process ($n$) | $g_1$ | $g_2$ | $h$ |
|---|---|---|---|
| I | $\xi v_{\mathbf{k}}e_{\mathbf{k}}-\eta u_{\mathbf{k}}$ | $\xi v_{\mathbf{k}'}e_{\mathbf{k}'}-\eta u_{\mathbf{k}'}$ | $u_{\mathbf{k}+\mathbf{q}}v_{\mathbf{k}'-\mathbf{q}}e_{-\mathbf{k}'+\mathbf{q}}+v_{\mathbf{k}+\mathbf{q}}u_{\mathbf{k}'-\mathbf{q}}e_{-\mathbf{k}-\mathbf{q}}$ |
| II | $\xi v_{\mathbf{k}}e_{\mathbf{k}}-\eta u_{\mathbf{k}}$ | $\xi u_{\mathbf{k}'+\mathbf{q}}e_{\mathbf{k}'+\mathbf{q}}-\eta v_{\mathbf{k}'+\mathbf{q}}$ | $u_{\mathbf{k}'}u_{\mathbf{k}+\mathbf{q}}e_{\mathbf{k}+\mathbf{q}}+v_{\mathbf{k}'}v_{\mathbf{k}+\mathbf{q}}e_{\mathbf{k}'}$ |
| III | $\xi u_{\mathbf{k}}e_{\mathbf{k}}-\eta v_{\mathbf{k}}$ | $\xi u_{\mathbf{k}'}e_{\mathbf{k}'}-\eta v_{\mathbf{k}'}$ | $v_{\mathbf{k}+\mathbf{q}}u_{\mathbf{k}'-\mathbf{q}}e_{-\mathbf{k}'+\mathbf{q}}+u_{\mathbf{k}+\mathbf{q}}v_{\mathbf{k}'-\mathbf{q}}e_{-\mathbf{k}-\mathbf{q}}$ |
| IV | $\xi v_{\mathbf{k}}e_{\mathbf{k}}-\eta u_{\mathbf{k}}$ | $\xi u_{\mathbf{k}'+\mathbf{q}}e_{\mathbf{k}'+\mathbf{q}}-\eta v_{\mathbf{k}'+\mathbf{q}}$ | $-(u_{\mathbf{k}'}v_{\mathbf{k}+\mathbf{q}}e_{-\mathbf{k}-\mathbf{q}}+v_{\mathbf{k}'}u_{\mathbf{k}+\mathbf{q}}e_{-\mathbf{k}'})$ |
| V | $\xi u_{\mathbf{k}}e_{\mathbf{k}}-\eta v_{\mathbf{k}}$ | $\xi v_{\mathbf{k}'+\mathbf{q}}e_{\mathbf{k}'+\mathbf{q}}-\eta u_{\mathbf{k}'+\mathbf{q}}$ | $-(u_{\mathbf{k}'}v_{\mathbf{k}+\mathbf{q}}e_{-\mathbf{k}'}+v_{\mathbf{k}'}u_{\mathbf{k}+\mathbf{q}}e_{-\mathbf{k}-\mathbf{q}})$ |
| VI | $\xi v_{\mathbf{k}}e_{\mathbf{k}}-\eta u_{\mathbf{k}}$ | $\xi v_{\mathbf{k}'}e_{\mathbf{k}'}-\eta u_{\mathbf{k}'}$ | $v_{\mathbf{k}+\mathbf{q}}u_{\mathbf{k}'-\mathbf{q}}e_{-\mathbf{k}'+\mathbf{q}}+u_{\mathbf{k}+\mathbf{q}}v_{\mathbf{k}'-\mathbf{q}}e_{-\mathbf{k}-\mathbf{q}}$ |

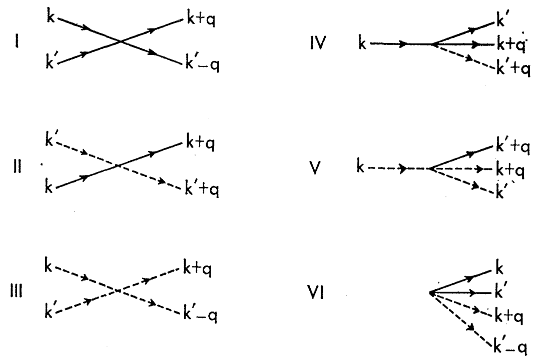


FIG. 3. Four-magnon processes for ferrimagnets. Here, real lines represent acoustical magnons and broken lines optical magnons. There are inverse processes to the processes given in these diagrams.

The contributions to $\Gamma_{\alpha\alpha}^{(2)}(\mathbf{k},\mathbf{k}')$ are the self-energies of four-magnon processes, the self-energies of two-magnon processes, and the diagonal terms of $H_2$. The process leading to the second contribution is a virtual emission or absorption of two magnons with the same wave vector, one of which is an $\alpha$ magnon and the other a $\beta$ magnon. The process comes from a part of $H_1$, which is given by (21). Now we write

$$\Gamma_{\alpha\alpha}^{(2)}(\mathbf{k},\mathbf{k}')=G_1+G_2+G_3\,, \tag{45}$$

where $G_1$, $G_2$, and $G_3$ are the first, second, and third contributions, respectively.

We consider first $G_1$, which comes from a second-order perturbation of the four-magnon process I, IV, and VI of $H_1$. The square of a matrix element, which appears in the numerator of the perturbation formula, is written

$$|V(n)|^2=\{V_1(n)\}^2+\tilde{V}_2(n)V_2(n)\,, \tag{46}$$

using (39) and (40). Thus we can divide $G_1$ into two parts,

$$G_1=G_1'+G_1''\,, \tag{47}$$

where

$$G_1'=-\tfrac{1}{2}(8N)^{-2}\sum_{\mathbf{q}}(X_{\mathrm{I}}/S_A-Y_{\mathrm{I}}/S_B)^2(\epsilon_{\mathbf{k}+\mathbf{q}\alpha}{}^0+\epsilon_{\mathbf{k}'-\mathbf{q}\alpha}{}^0-\epsilon_{\mathbf{k}\alpha}{}^0-\epsilon_{\mathbf{k}'\alpha}{}^0)-\tfrac{1}{2}(8N)^{-2}\sum_{\mathbf{q}}(X_{\mathrm{VI}}/S_A-Y_{\mathrm{VI}}/S_B)^2$$
$$\times(\epsilon_{\mathbf{k}+\mathbf{q}\beta}{}^0+\epsilon_{\mathbf{k}'-\mathbf{q}\beta}{}^0+\epsilon_{\mathbf{k}\alpha}{}^0+\epsilon_{\mathbf{k}'\alpha}{}^0)-2(8N)^{-2}\sum_{\mathbf{q}}(X_{\mathrm{IV}}/S_A-Y_{\mathrm{IV}}/S_B)^2(\epsilon_{\mathbf{k}+\mathbf{q}\alpha}{}^0+\epsilon_{\mathbf{k}'+\mathbf{q}\beta}{}^0+\epsilon_{\mathbf{k}'\alpha}{}^0-\epsilon_{\mathbf{k}\alpha}{}^0)\,; \tag{48}$$

$$G_1''=-\tfrac{1}{2}\sum_{\mathbf{q}}\frac{\tilde{V}_2(\mathrm{I})V_2(\mathrm{I})}{\epsilon_{\mathbf{k}+\mathbf{q}\alpha}{}^0+\epsilon_{\mathbf{k}'-\mathbf{q}\alpha}{}^0-\epsilon_{\mathbf{k}'\alpha}{}^0-\epsilon_{\mathbf{k}\alpha}{}^0}-\tfrac{1}{2}\sum_{\mathbf{q}}\frac{\tilde{V}_2(\mathrm{VI})V_2(\mathrm{VI})}{\epsilon_{\mathbf{k}+\mathbf{q}\beta}{}^0+\epsilon_{\mathbf{k}'-\mathbf{q}\beta}{}^0+\epsilon_{\mathbf{k}\alpha}{}^0+\epsilon_{\mathbf{k}'\alpha}{}^0}-2\sum_{\mathbf{q}}\frac{\tilde{V}_2(\mathrm{IV})V_2(\mathrm{IV})}{\epsilon_{\mathbf{k}+\mathbf{q}\alpha}{}^0+\epsilon_{\mathbf{k}'+\mathbf{q}\beta}{}^0+\epsilon_{\mathbf{k}'\alpha}{}^0-\epsilon_{\mathbf{k}\alpha}{}^0}\,. \tag{49}$$

Here we have used Table I. The respective last terms of (48) and (49) are assumed to be symmetrized with respect to $\mathbf{k}$ and $\mathbf{k}'$, although no symmetrized form was included for the sake of brevity.

The last term of (48) comes from Process IV, and it includes $\mathbf{k}'+\mathbf{q}$ but not $\mathbf{k}'-\mathbf{q}$. However, the energy shift of magnons is given by $\sum_{\mathbf{k}'}\Gamma_{\alpha\alpha}^{(2)}(\mathbf{k},\mathbf{k}')\bar{n}_{\mathbf{k}'\alpha}$; hence the results remain unaltered if we replace $\mathbf{k}'$ by $-\mathbf{k}'$. In this way, $G_1'$ is written effectively as

$$G_1'=-4(8NS_AS_B)^{-2}(\gamma_0JS)/(f_{\mathbf{k}}f_{\mathbf{k}'})\sum_{\mathbf{q}}f_{\mathbf{q}}^{-1}[S_B{}^2(1+f_{\mathbf{k}})(1+f_{\mathbf{k}'})(3-f_{\mathbf{k}}-f_{\mathbf{k}'}-f_{\mathbf{q}}{}^2)$$
$$+S_A{}^2(1-f_{\mathbf{k}})(1-f_{\mathbf{k}'})(3+f_{\mathbf{k}}+f_{\mathbf{k}'}-f_{\mathbf{q}}{}^2)-6S^2(1-f_{\mathbf{k}}{}^2)(1-f_{\mathbf{k}'}{}^2)(1-f_{\mathbf{q}}{}^2)]\,, \tag{50}$$

where we replaced

$$\{(S_AS_B)^{1/2}/(\gamma_0S)\}\gamma_{\mathbf{k}+\mathbf{k}'-\mathbf{q}}=\mathrm{sgn}\gamma_{\mathbf{k}+\mathbf{k}'-\mathbf{q}}(1-f_{\mathbf{k}+\mathbf{k}'-\mathbf{q}}{}^2)^{1/2}$$

by

$$\{(S_AS_B)^{1/2}/(\gamma_0{}^3S)\}\gamma_{\mathbf{k}}\gamma_{\mathbf{k}'}\gamma_{\mathbf{q}}$$

for the same reason as given by (28).

Now, $G_1''$ vanishes if any one of $\mathbf{k}$ and $\mathbf{k}'$ goes to the long-wavelength limit, because $\tilde{V}_2V_2$ for a relevant process vanishes at the same limit. This is not the case for $G_1'$, whose long-wavelength limit should be cancelled by the corresponding limit value of $G_2+G_3$. Before going to an evaluation of $G_1''$, we shall look into the cancellation mentioned above. As will be seen later, $G_2$ vanishes only at the long-wavelength limit of both $\mathbf{k}$ and $\mathbf{k}'$. Thus $G_1'+G_3$ vanishes only at the same limit of both $\mathbf{k}$ and $\mathbf{k}'$.

The diagonal term of $H_2$ is written from (8).

$$G_3=4(8NS_AS_B)^{-2}(\gamma_0JS)/(f_{\mathbf{k}}f_{\mathbf{k}'})\sum_{\mathbf{q}}\{S_B{}^2(1+f_{\mathbf{k}})(1+f_{\mathbf{k}'})[3(3-f_{\mathbf{k}}-f_{\mathbf{k}'}+f_{\mathbf{q}})(1-f_{\mathbf{q}})+(2-f_{\mathbf{k}}-f_{\mathbf{k}'})f_{\mathbf{q}}]$$
$$+S_A{}^2(1-f_{\mathbf{k}})(1-f_{\mathbf{k}'})[3(3+f_{\mathbf{k}}+f_{\mathbf{k}'}+f_{\mathbf{q}})(1-f_{\mathbf{q}})+(2+f_{\mathbf{k}}+f_{\mathbf{k}'})f_{\mathbf{q}}]$$
$$-4S_AS_B(1-f_{\mathbf{q}})[2-f_{\mathbf{k}}{}^2-f_{\mathbf{k}'}{}^2+(1-f_{\mathbf{k}}f_{\mathbf{k}'})(1+f_{\mathbf{q}})]-6S^2(1-f_{\mathbf{k}}{}^2)(1-f_{\mathbf{k}'}{}^2)(1-f_{\mathbf{q}}{}^2)]\,. \tag{51}$$

Taking the sum of (50) and (51), we get

$$G_1'+G_3=-2[2N(1-\alpha^2)]^{-2}(\gamma_0J/S)/(f_{\mathbf{k}}f_{\mathbf{k}'})$$
$$\times\sum_{\mathbf{q}}f_{\mathbf{q}}^{-1}(1-f_{\mathbf{q}})\{\alpha[(1-f_{\mathbf{k}'}{}^2)(f_{\mathbf{k}}-\alpha)+(1-f_{\mathbf{k}}{}^2)(f_{\mathbf{k}'}-\alpha)]-(1+f_{\mathbf{q}})(f_{\mathbf{k}}-\alpha)(f_{\mathbf{k}'}-\alpha)\}\,, \tag{52}$$

which has the required form.

A second-order perturbation of the two-magnon process of $H_1$ gives (see Appendix B)

$$G_2=2\alpha^2[2N(1-\alpha^2)]^{-2}(\gamma_0J/S)/(f_{\mathbf{k}}f_{\mathbf{k}'})\times\sum_{\mathbf{q}} f_{\mathbf{q}}^{-1}\{\alpha[(f_{\mathbf{k}}-\alpha)(1-f_{\mathbf{k}'}^2)/f_{\mathbf{k}'}^2+(f_{\mathbf{k}'}-\alpha)(1-f_{\mathbf{k}}^2)/f_{\mathbf{k}}^2](1-f_{\mathbf{q}})-(f_{\mathbf{k}}-\alpha)(f_{\mathbf{k}'}-\alpha)(1-f_{\mathbf{q}}^2)/f_{\mathbf{q}}^2\}. \quad (53)$$

From (52) and (53), we obtain

$$G_1'+G_2+G_3=-(\gamma_0J/S)[2N(1-\alpha^2)^2]^{-1}(f_{\mathbf{k}}-\alpha)(f_{\mathbf{k}'}-\alpha)/(f_{\mathbf{k}}f_{\mathbf{k}'})\{\alpha[(f_{\mathbf{k}}+\alpha)(1-f_{\mathbf{k}}^2)/f_{\mathbf{k}}^2+(f_{\mathbf{k}'}+\alpha)(1-f_{\mathbf{k}'}^2)/f_{\mathbf{k}'}^2][N^{-1}\textstyle\sum_{\mathbf{q}}(1-f_{\mathbf{q}})/f_{\mathbf{q}}]-N^{-1}\textstyle\sum_{\mathbf{q}}(f_{\mathbf{q}}^2-\alpha^2)(1-f_{\mathbf{q}}^2)/f_{\mathbf{q}}^3\}, \quad (54)$$

which vanishes at the long-wavelength of any one of $\mathbf{k}$ and $\mathbf{k}'$ as required. In a long-wavelength approximation, (54) becomes

$$G_1'+G_2+G_3\cong-(\gamma_0J/S)/\{2N(\gamma_0\alpha^2)^2\}\{4(1-\alpha^2)[N^{-1}\textstyle\sum_{\mathbf{q}}(1-f_{\mathbf{q}})/f_{\mathbf{q}}]-N^{-1}\textstyle\sum_{\mathbf{q}}(f_{\mathbf{q}}^2-\alpha^2)(1-f_{\mathbf{q}}^2)/f_{\mathbf{q}}^3\}(ka)^2(k'a)^2. \quad (55)$$

We shall now evaluate $G_1''$ given by (49). We pick up the first two terms of (49) to evaluate in a long-wavelength approximation. The result is a sum of the following two terms:

$$-\{J/(2NS)\}\cdot\{(1-\alpha^2)/\alpha^2\}(ka)^2(k'a)^2\{(\gamma_0\alpha^2)^{-1}N^{-1}\textstyle\sum_{\mathbf{q}}(1-f_{\mathbf{q}}^2)/f_{\mathbf{q}}+(1/3)(\gamma_0a)^{-2}N^{-1}\textstyle\sum_{\mathbf{q}}(\nabla\gamma_{\mathbf{q}}\cdot\nabla\gamma_{\mathbf{q}})/f_{\mathbf{q}}^3\}, \quad (56a)$$

and

$$-\{J/(36N\gamma_0S)\}\{(1-\alpha^2)/\alpha\}^2(ka)^2(k'a)^2(\gamma_0a^2)^{-2}N^{-1}\sum_{\mathbf{q}}\frac{\gamma_{\mathbf{q}}^2\{\sum_{\mu\nu}(\nabla_\mu\nabla_\nu\gamma_{\mathbf{q}})^2\}}{f_{\mathbf{q}}(f_{\mathbf{q}}^2-\alpha^2)}. \quad (56b)$$

(See Appendix C.) Here $\nabla_\mu=\partial/\partial q_\mu$, and $q_\mu$ is a component of a vector $\mathbf{q}$.

Finally we evaluate the last term of (49), where the result is given in Appendix D. Thus $\Gamma_{\alpha\alpha}^{(2)}$, given by (45), becomes

$$\Gamma_{\alpha\alpha}^{(2)}(\mathbf{k},\mathbf{k}')=-\frac{Q}{(1-\alpha^2)S}\Gamma_{\alpha\alpha}^{(1)}(\mathbf{k},\mathbf{k}'), \quad (57)$$

$$Q=\frac{1}{N}\sum\bigg\{\frac{1}{6}\frac{9-25\alpha^2}{1-\alpha^2}\cdot\frac{1}{f_{\mathbf{q}}}-2+\frac{1+\alpha^2}{2(1-\alpha^2)}f_{\mathbf{q}}+\frac{5}{3}\frac{\alpha^2}{1-\alpha^2}\frac{1}{f_{\mathbf{q}}^3}+\frac{\alpha^2}{6}\bigg[\frac{1}{3}-5\frac{1-\alpha^2}{f_{\mathbf{q}}^2}\Big(\frac{\gamma_{\mathbf{q}}}{\gamma_0}\Big)^2\bigg]\frac{1}{\gamma_0a^2}\frac{(\nabla\gamma_{\mathbf{q}}\cdot\nabla\gamma_{\mathbf{q}})}{f_{\mathbf{q}}^3}+\frac{\alpha^2}{36}\frac{f_{\mathbf{q}}^{-1}(\gamma_{\mathbf{q}}/\gamma_0)^2}{1-(\gamma_{\mathbf{q}}/\gamma_0)^2}\frac{1}{a^4}\textstyle\sum_{\mu,\nu}(\nabla_\mu\nabla_\nu\gamma_{\mathbf{q}})^2+\frac{\alpha^2}{36}\frac{1-\alpha^2}{f_{\mathbf{q}}^5}\bigg[1+5\frac{1-\alpha^2}{f_{\mathbf{q}}^2}\Big(\frac{\gamma_{\mathbf{q}}}{\gamma_0}\Big)^2\bigg]\frac{(\nabla\gamma_{\mathbf{q}}\cdot\nabla\gamma_{\mathbf{q}})^2}{\gamma_0^2a^4}\bigg\}, \quad (58)$$

where $\Gamma_{\alpha\alpha}^{(1)}$ is given by (44), and we used (45), (47), (55), (56a, b), and the result of Appendix D.

Estimates of the integrals needed for an estimation of $Q$ are given in Table III, whence we estimate $Q$ to be 0.15 for the CsCl-type structure, with $\alpha=\frac{1}{3}$. Thus the second-order effect is small at low temperatures.

### VI. TEMPERATURE BEHAVIOR OF MAGNON FREQUENCIES

As was shown in the preceding section, the second-order shift is small, at least in low-temperature regions, so we now may predict the temperature behavior of magnon frequencies, based on the first-order shift.

We note first that population numbers are given by

$$\bar{n}_{\mathbf{k}\alpha}=[\exp(\epsilon_{\mathbf{k}\alpha}/k_BT)-1]^{-1},\quad \bar{n}_{\mathbf{k}\beta}=[\exp(\epsilon_{\mathbf{k}\beta}/k_BT)-1]^{-1}, \quad (59)$$

where $\epsilon_{\mathbf{k}\alpha}$ and $\epsilon_{\mathbf{k}\beta}$ are magnon energies at a finite temperature. Equation (59) is a direct consequence of the commutation relations

$$[\alpha_{\mathbf{k}},\alpha_{\mathbf{k}}^*]=[\beta_{\mathbf{k}},\beta_{\mathbf{k}}^*]=1, \quad (60)$$

which are derived from $[a_j,a_{j'}^*]=\delta_{jj'}$ and $[b_l,b_{l'}^*]=\delta_{ll'}$, using (5) and (12). We can verify (59) easily by taking a thermal average of (60) multiplied by $\exp(-H/k_BT)$, where we use a Hartree approximation.

First we approximate $\epsilon_{\mathbf{k}\alpha}$ and $\epsilon_{\mathbf{k}\beta}$ in (59) by their temperature-independent parts, $\epsilon_{\mathbf{k}\alpha}^0$ and $\epsilon_{\mathbf{k}\beta}^0$, without zero-point corrections. The resulting population numbers are denoted by $\bar{n}_{\mathbf{k}\alpha}^0$ and $\bar{n}_{\mathbf{k}\beta}^0$. In this approximation, from (27) we get

$$\Delta\epsilon_{\mathbf{k}\alpha}^{(1)}=\textstyle\sum_{\mathbf{k}'}\Gamma_{\alpha\alpha}(\mathbf{k},\mathbf{k}')\bar{n}_{\mathbf{k}'\alpha}^0+\sum_{\mathbf{k}'}\Gamma_{\alpha\beta}(\mathbf{k},\mathbf{k}')\bar{n}_{\mathbf{k}'\beta}^0,\quad \Delta\epsilon_{\mathbf{k}\beta}^{(1)}=\sum_{\mathbf{k}'}\Gamma_{\beta\alpha}(\mathbf{k},\mathbf{k}')\bar{n}_{\mathbf{k}'\alpha}^0+\sum_{\mathbf{k}'}\Gamma_{\beta\beta}(\mathbf{k},\mathbf{k}')\bar{n}_{\mathbf{k}'\beta}^0. \quad (61)$$

This is a fairly good approximation at low temperatures. We have already given the low-temperature characteristic of frequency shifts on the same basis (Sec. III). The approximation becomes less accurate at higher temperatures; still, it will be suggestive to predict frequency shifts at high temperatures by the use of the same approximation. Now $\bar{n}_{\mathbf{k}\alpha}^0$ and $\bar{n}_{\mathbf{k}\beta}^0$ may be approximated by

$$\bar{n}_{\mathbf{k}\alpha}^0\cong x/(f_{\mathbf{k}}-\alpha)-\tfrac{1}{2};\quad \bar{n}_{\mathbf{k}\beta}^0\cong x/(f_{\mathbf{k}}+\alpha)-\tfrac{1}{2}, \quad (62)$$

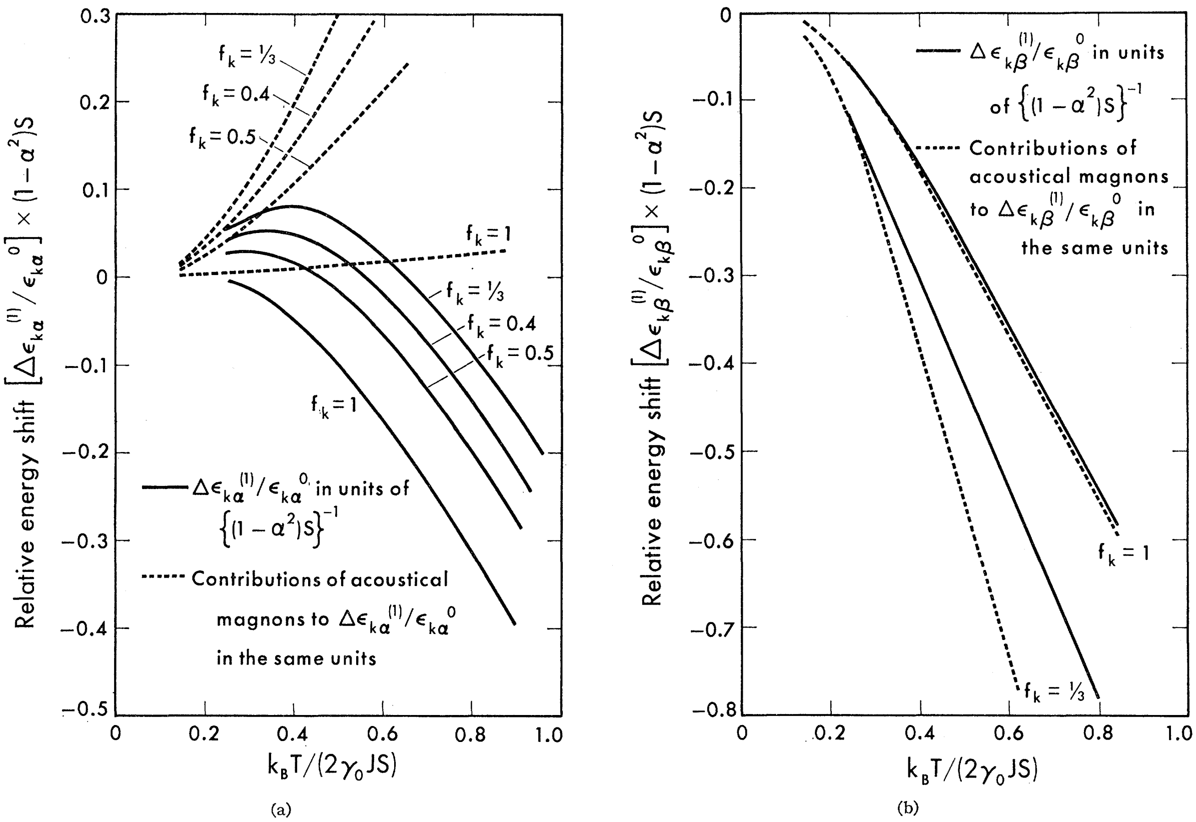


FIG. 4. Temperature dependence of relative energy shifts: (a) for acoustical branch, and (b) for optical branch. No effect of population change due to the energy shift is taken into account. There $f_k=\frac{1}{3}$ and 1.0 correspond to the long- and short-wavelength limits, respectively, and acoustical magnons with $f_k=0.4$ and 0.5 have energies equal to 10% and 25%, respectively of the full width of the acoustical band.

using (10), where

$$x=k_BT/(2\gamma_0 JS). \tag{63}$$

Equations (61) are the first two terms of the power series of population numbers in $1/x$. The series is convergent for $x>2/3\pi$ (the top of the $\beta$ band) and $x>1/3\pi$ (the top of the $\alpha$ band). Substituting (62) into (61) and using (29) with (29a), we have

$$\begin{aligned}\Delta\epsilon_{k\alpha}^{(1)}/\epsilon_{k\alpha}^{0}&=\{(1-\alpha^2)S\}^{-1}(\varphi_1/f_k-\varphi_2);\\ \Delta\epsilon_{k\beta}^{(1)}/\epsilon_{k\beta}^{0}&=-\{(1-\alpha^2)S\}^{-1}(\varphi_1/f_k+\varphi_2),\end{aligned} \tag{64}$$

where

$$\begin{aligned}\varphi_1&\sim(\alpha/2)(N^{-1}\textstyle\sum_k f_k^{-1});\\ \varphi_2&\sim x-(\tfrac{1}{2})(N^{-1}\textstyle\sum_k f_k).\end{aligned} \tag{65}$$

We see from the above expressions that $\Delta\epsilon_{k\alpha}^{(1)}$ and $\Delta\epsilon_{k\beta}^{(1)}$ have negative temperature coefficients and that temperature coefficients of the relative shift approach each other with increasing temperature.

As mentioned in Sec. III, $\Delta\epsilon_{k\alpha}^{(1)}$ has a positive temperature coefficient at low temperatures. Thus $\Delta\epsilon_{k\alpha}^{(1)}$ has a maximum at a rather low temperature. The temperature at which the maximum appears depends on the wave vector associated with the $\alpha$ magnon, and the temperatures decrease with increasing $k$. This feature is shown in Fig. 4, where we have plotted relative shifts as a function of $x$ for both $\alpha$ and $\beta$ magnons with several energies. These were obtained by the use of an IBM computer, taking into account many more terms in the series given by (62). Contributions of thermal $\alpha$ magnons to the relative shift are also given in the same figure. They increase with increasing temperature for $\alpha$ magnons. If we subtract the acoustical contributions from the relative shifts, we obtain the optical contributions. The thermal excitations of optical magnons decrease the energy of $\alpha$ magnons. This effect is more considerable at higher temperatures because of the increased populations of $\beta$ magnons. The weak temperature dependence of $\alpha$-magnon energies is a result of the cancellation of the two competing effects mentioned above. On the other hand, for $\beta$ magnons, the relative shifts decrease rapidly, because the $\alpha$-$\beta$ interaction is stronger with a negative sign than the $\beta$-$\beta$ interaction with a positive sign, and $\alpha$ magnons are more populated than $\beta$ magnons. As shown in Fig. 4, the most rapid decrease of relative shifts occurs near the exchange-resonance mode, with $f_k=\alpha$.

Next we shall consider the effect of population change due to energy shifts. This is accomplisehd by solving (27) with (59), where $\epsilon_{k\alpha}=\epsilon_{k\alpha}^{0}+\Delta\epsilon_{k\alpha}$ and $\epsilon_{k\beta}=\epsilon_{k\beta}^{0}$

TABLE III. Estimates of some integrals. Estimates are given for the CsCl-type structure with $\alpha=\frac{1}{3}$, where

$$\gamma_{\mathbf{k}}/\gamma_0=\cos(k_xa/2)\cos(k_ya/2)\cos(k_za/2)$$

and $N^{-1}\Sigma_{\mathbf{k}}(\cdots)$ represents

$$(2\pi/a)^{-3}\int\int\int_{-\pi/a}^{\pi/a}dk_xdk_ydk_z(\cdots).$$

| | | | | |
|---|---|---|---|---|
| Integral | $N^{-1}\Sigma_{\mathbf{k}}f_{\mathbf{k}}$ | $N^{-1}\Sigma_{\mathbf{k}}f_{\mathbf{k}}^{-1}$ | $N^{-1}\Sigma_{\mathbf{k}}f_{\mathbf{k}}^{-3}$ | $N^{-1}(\gamma_0a)^{-2}\Sigma_{\mathbf{k}}(\nabla\gamma_{\mathbf{k}}\cdot\nabla\gamma_{\mathbf{k}})/f_{\mathbf{k}}^3$ |
| Estimate | 0.93688 | 1.08779 | 1.42885 | 0.127 |
| Integral | $N^{-1}(\gamma_0a)^{-2}\Sigma_{\mathbf{k}}\frac{(\nabla\gamma_{\mathbf{k}}\cdot\nabla\gamma_{\mathbf{k}})}{f_{\mathbf{k}}^3}$ | $N^{-1}(\gamma_0a)^{-4}\Sigma_{\mathbf{k}}\frac{(\nabla\gamma_{\mathbf{k}}\cdot\nabla\gamma_{\mathbf{k}})^2}{f_{\mathbf{k}}^5}$ | $N^{-1}(\gamma_0a)^{-4}\Sigma_{\mathbf{k}}\frac{(\nabla\gamma_{\mathbf{k}}\cdot\nabla\gamma_{\mathbf{k}})^2}{f_{\mathbf{k}}^7}$ | $N^{-1}(\gamma_0a)^{-2}\Sigma_{\mathbf{k}}\Sigma_{\mu,\nu}\frac{f_{\mathbf{k}}^{-1}(\gamma_{\mathbf{k}}/\gamma)^2}{1-(\gamma_{\mathbf{k}}/\gamma_0)^2}\times(\nabla_\mu\nabla_\nu\gamma_{\mathbf{k}})^2$ |
| Estimate | 0.181 | 0.0201 | 0.0292 | 0.11 |

$+\Delta\epsilon_{\mathbf{k}\beta}$. The same problem has been studied for ferromagnets and antiferromagnets,[11] where a single parameter is estimated. This parameter merely gives the relative shift, which is the same for all modes. This is not the case for ferrimagnets, where we need another parameter to obtain the solution, for which we use the method of successive approximations. We start with

$$\bar{n}_{\mathbf{k}\alpha}=\bar{n}_{\mathbf{k}\alpha}^0+\Delta\bar{n}_{\mathbf{k}\alpha}^{(1)}+\cdots,\quad \bar{n}_{\mathbf{k}\beta}=\bar{n}_{\mathbf{k}\beta}^{(0)}+\Delta\bar{n}_{\mathbf{k}\beta}^{(1)}+\cdots. \tag{66}$$

Here $\Delta\bar{n}_{\mathbf{k}\alpha}^{(1)}$ and $\Delta\bar{n}_{\mathbf{k}\beta}^{(1)}$ represent population changes linear in $\Delta\epsilon_{\mathbf{k}\alpha}^{(1)}$ and $\Delta\epsilon_{\mathbf{k}\beta}^{(1)}$ obtained from the zeroth approximation of population numbers $\bar{n}_{\mathbf{k}\alpha}^0$ and $\bar{n}_{\mathbf{k}\beta}^0$. If we substitute (66) into (27) with (59), the second approximation of energy shifts is obtained:

$$\Delta\epsilon_{\mathbf{k}\alpha}^{(2)}=\sum_{\mathbf{k}'}\Gamma_{\alpha\alpha}(\mathbf{k},\mathbf{k}')\Delta\bar{n}_{\mathbf{k}'\alpha}^{(1)}+\sum_{\mathbf{k}'}\Gamma_{\alpha\beta}(\mathbf{k},\mathbf{k}')\Delta\bar{n}_{\mathbf{k}'\beta}^{(1)}, \tag{67}$$
$$\Delta\epsilon_{\mathbf{k}\beta}^{(2)}=\sum_{\mathbf{k}'}\Gamma_{\beta\alpha}(\mathbf{k},\mathbf{k}')\Delta\bar{n}_{\mathbf{k}'\alpha}^{(1)}+\sum_{\mathbf{k}'}\Gamma_{\beta\beta}(\mathbf{k},\mathbf{k}')\Delta\bar{n}_{\mathbf{k}'\beta}^{(1)}.$$

The third approximation of the shifts are expressed in terms of $\Delta\bar{n}_{\mathbf{k}\alpha}^{(2)}$ and $\Delta\bar{n}_{\mathbf{k}\beta}^{(2)}$, which consist of population changes quadratic in $\Delta\epsilon_{\mathbf{k}\alpha}^{(1)}$ and $\Delta\epsilon_{\mathbf{k}\beta}^{(1)}$ and those linear in $\Delta\epsilon_{\mathbf{k}\alpha}^{(2)}$ and $\Delta\epsilon_{\mathbf{k}\beta}^{(2)}$. Thus, we have series expansions of $\Delta\epsilon_{\mathbf{k}\alpha}$ and $\Delta\epsilon_{\mathbf{k}\beta}$ with respect to $[(1-\alpha^2)S]^{-1}$. We have plotted the results in Fig. 5 for $S=\frac{3}{4}$, where we have taken into account $\Delta\epsilon_{\mathbf{k}\alpha}$ and $\Delta\epsilon_{\mathbf{k}\beta}$ up to the third approximation.

The self-consistent solution is exactly obtained from evaluations of two parameters, $p$ and $q$

$$p=-M\{\sum_{\mathbf{k}'}(f_{\mathbf{k}'}-\alpha)\bar{n}_{\mathbf{k}'\alpha}+\sum_{\mathbf{k}'}(f_{\mathbf{k}'}+\alpha)\bar{n}_{\mathbf{k}'\beta}\},$$
$$q=M\alpha\{-\sum_{\mathbf{k}'}[1-(\alpha/f_{\mathbf{k}'})]\bar{n}_{\mathbf{k}'\alpha}+\sum_{\mathbf{k}'}[1+(\alpha/f_{\mathbf{k}'})]\bar{n}_{\mathbf{k}'\beta}\}, \tag{68}$$

which satisfy

$$\begin{pmatrix}\Delta\epsilon_{\mathbf{k}\alpha}\\ \Delta\epsilon_{\mathbf{k}\beta}\end{pmatrix}=(pf_{\mathbf{k}}+q/f_{\mathbf{k}})\begin{pmatrix}-\\+\end{pmatrix}(p\alpha+q/\alpha) \tag{69}$$

as easily shown by (27) and (29) with (29a). The resulting solution for $S=\frac{3}{4}$ is given in Fig. 5. The solution disappears beyond a temperature $k_BT/(2\gamma_0JS)=0.395$. This may be very close to the Curie temperature, as expected from comparisons of the corresponding results for ferro- and antiferromagnets[11] with accurate estimates of the transition temperatures. It may be noted that a sharp decrease in magnon energy occurs very near the

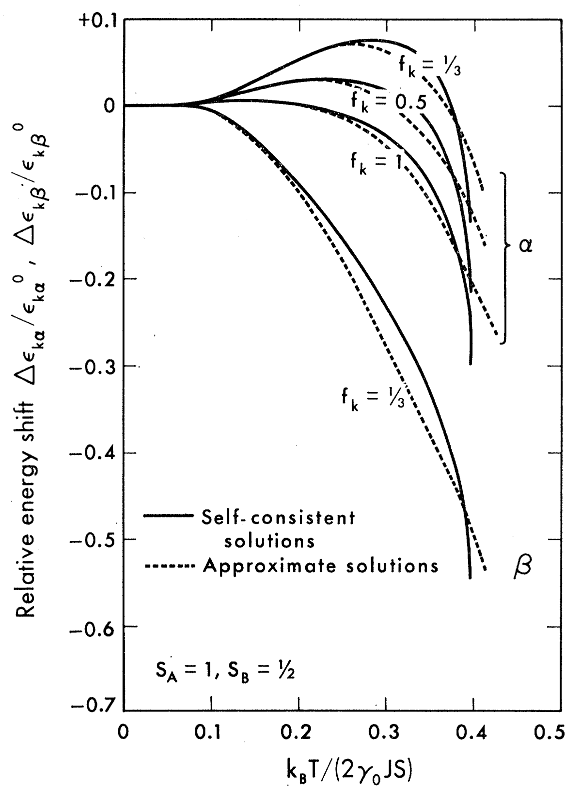


FIG. 5. Temperature dependence of relative energy shifts ($S=\frac{3}{4}$). Population changes due to the energy shift are taken into account. The Curie point may be around $k_BT/(2\gamma_0JS)=0.4$. Low-temperature parts of the curves are drawn by use of the following results: (1) a high-temperature expansion without contribution of thermal optical magnons; (2) a low-temperature expansion.

[11] M. Bloch, Phys. Rev. Letters 9, 286 (1962); J. Appl. Phys. 34, 1151 (1963).

temperature mentioned. Still, a large part of the magnon energy remains at that temperature; another notable result.

It may be difficult to predict what really happens close to the Curie point from the present treatment, because our Hamiltonian has been truncated. The contribution of higher order terms to the frequency shift is small at low temperatures. As shown in the solution of (27) with (59) by the method of successive approximation, the frequency shift is expressed by a series in $1/S$. The second term in the series is of the same order as the first term to come from the second-order effect of the Hamiltonian, in which the latter is quadratic in population numbers.

## VII. CONCLUSION

We have studied the temperature dependence of magnon frequencies in ferrimagnets, based on a two-sublattice model.

The primary term of magnon interactions, which is of the order $(1/S)^0$, has the following nature. The interaction energy is positive in sign between two acoustical magnons and between two optical magnons, whereas it is negative between an acoustical and an optical magnon. Thus, in low-temperature regions, the magnon frequency increases for the acoustical branch and decreases for the optical branch, because thermal magnons are dominantly acoustical in low-temperature regions. Temperature variations obey the $T^{5/2}$ law. It is also noted that the increase of relative shifts is more notable for acoustical magnons with longer wavelength.

In high-temperature regions, acoustical-magnon frequencies cease to rise and then decrease with increasing temperature because of the magnon populations in the optical branch. The decrease will begin at lower temperatures for acoustical magnons with shorter wavelength. Moreover, the decrease is enhanced by population change due to the first-order shift, because optical-magnon frequency decrease considerably; hence the increase of optical-magnon population is enhanced by a lowering of the frequency.

These predictions are based on the first-order shift of magnon frequencies. The second-order shift has proved to be small at low temperatures. However, the higher order effect will become appreciable near the Curie point. Our treatment may predict correctly behaviors up to the temperature at which the largest relative shift attains, say $-0.4$.

## ACKNOWLEDGMENTS

The authors wish to thank Professor C. Kittel for his valuable comments and for the hospitality at the University of California. We are indebted to Arthur Miller for his continual help in computer programming. One of the authors (T.N.) wishes to thank Professor A. M. Portis for the hospitality extended to him.

## APPENDIX A

The matrix element of Process I shown in Fig. 2 is given by a coefficient of $\alpha_{\mathbf{k}+\mathbf{q}}{}^*\alpha_{\mathbf{k}'-\mathbf{q}}{}^*\alpha_{\mathbf{k}}\alpha_{\mathbf{k}'}$, if we substitute (12) into $H_1$ of (7). This coefficient is written

$$V(\mathrm{I})=N^{-1}J(L_1-L_2); \tag{A1}$$

$$L_1=(S_AS_B)^{-1/2}[S_Bu_{\mathbf{k}}u_{\mathbf{k}'}(u_{\mathbf{k}+\mathbf{q}}v_{\mathbf{k}'-\mathbf{q}}\gamma_{\mathbf{k}'-\mathbf{q}}+u_{\mathbf{k}'-\mathbf{q}}v_{\mathbf{k}+\mathbf{q}}\gamma_{\mathbf{k}+\mathbf{q}})+S_Av_{\mathbf{k}}v_{\mathbf{k}'}(u_{\mathbf{k}+\mathbf{q}}v_{\mathbf{k}'-\mathbf{q}}\gamma_{\mathbf{k}+\mathbf{q}}+u_{\mathbf{k}'-\mathbf{q}}v_{\mathbf{k}+\mathbf{q}}\gamma_{\mathbf{k}'-\mathbf{q}})$$
$$+S_Bu_{\mathbf{k}+\mathbf{q}}u_{\mathbf{k}'-\mathbf{q}}(u_{\mathbf{k}}v_{\mathbf{k}'}\gamma_{\mathbf{k}'}+u_{\mathbf{k}'}v_{\mathbf{k}}\gamma_{\mathbf{k}})+S_Av_{\mathbf{k}+\mathbf{q}}v_{\mathbf{k}'-\mathbf{q}}(u_{\mathbf{k}'}v_{\mathbf{k}}\gamma_{\mathbf{k}'}+u_{\mathbf{k}}v_{\mathbf{k}'}\gamma_{\mathbf{k}})]; \tag{A2}$$

$$L_2=2u_{\mathbf{k}}v_{\mathbf{k}'}(u_{\mathbf{k}+\mathbf{q}}v_{\mathbf{k}'-\mathbf{q}}\gamma_{\mathbf{q}}+u_{\mathbf{k}'-\mathbf{q}}v_{\mathbf{k}+\mathbf{q}}\gamma_{\mathbf{k}'-\mathbf{k}-\mathbf{q}})+2u_{\mathbf{k}'}v_{\mathbf{k}}(u_{\mathbf{k}+\mathbf{q}}v_{\mathbf{k}'-\mathbf{q}}\gamma_{\mathbf{k}'-\mathbf{k}-\mathbf{q}}+v_{\mathbf{k}+\mathbf{q}}u_{\mathbf{k}'-\mathbf{q}}\gamma_{\mathbf{q}}). \tag{A3}$$

Using (13), we have

$$L_1=\{\gamma_0/[(1-\alpha^2)S]\}\{S_B(4-f_{\mathbf{k}}-f_{\mathbf{k}'}-f_{\mathbf{k}+\mathbf{q}}-f_{\mathbf{k}'-\mathbf{q}})u_{\mathbf{k}}u_{\mathbf{k}'}u_{\mathbf{k}+\mathbf{q}}u_{\mathbf{k}'-\mathbf{q}}+S_A(4+f_{\mathbf{k}}+f_{\mathbf{k}'}+f_{\mathbf{k}+\mathbf{q}}+f_{\mathbf{k}'-\mathbf{q}})v_{\mathbf{k}}v_{\mathbf{k}'}v_{\mathbf{k}+\mathbf{q}}v_{\mathbf{k}'-\mathbf{q}}\}, \tag{A4}$$

which is divided into two parts:

$$\{\gamma_0/[(1-\alpha^2)S]\}(f_{\mathbf{k}+\mathbf{q}}+f_{\mathbf{k}'-\mathbf{q}}-f_{\mathbf{k}}-f_{\mathbf{k}'})(S_Bu_{\mathbf{k}}u_{\mathbf{k}'}u_{\mathbf{k}+\mathbf{q}}u_{\mathbf{k}'-\mathbf{q}}-S_Av_{\mathbf{k}}v_{\mathbf{k}'}v_{\mathbf{k}+\mathbf{q}}v_{\mathbf{k}'-\mathbf{q}}), \tag{A5}$$

and

$$2\gamma_0/[(1-\alpha^2)S]\{S_B(2-f_{\mathbf{k}+\mathbf{q}}-f_{\mathbf{k}'-\mathbf{q}})u_{\mathbf{k}}u_{\mathbf{k}'}u_{\mathbf{k}+\mathbf{q}}u_{\mathbf{k}'-\mathbf{q}}+S_A(2+f_{\mathbf{k}+\mathbf{q}}+f_{\mathbf{k}'-\mathbf{q}})v_{\mathbf{k}}v_{\mathbf{k}'}v_{\mathbf{k}+\mathbf{q}}v_{\mathbf{k}'-\mathbf{q}}\}. \tag{A6}$$

The first part (A5) leads to $V_1(\mathrm{I})$, as given in Table I. A sum of (A6) and (A3) is factorized as shown in Table II, where (A6) is rewritten in the same form as the first two terms of (A2) with the addition of a factor of 2.

## APPENDIX B

Substituting (12) into (21) and picking up terms with $\alpha_{\mathbf{k}}\beta_{\mathbf{k}}+a_{\mathbf{k}}{}^*\beta_{\mathbf{k}}{}^*$, we obtain

$$-(2\gamma_0J/N)\textstyle\sum_{\mathbf{k}'}\{A_{\mathbf{k}\mathbf{k}'}+B_{\mathbf{k}\mathbf{k}'}n_{\mathbf{k}'\alpha}+C_{\mathbf{k}\mathbf{k}'}n_{\mathbf{k}'\beta}\}(\alpha_{\mathbf{k}}\beta_{\mathbf{k}}+\alpha_{\mathbf{k}}{}^*\beta_{\mathbf{k}}{}^*), \tag{B1}$$

where

$$A_{\mathbf{kk}'}=(u_{\mathbf{k}}^2+v_{\mathbf{k}}^2)\{(1-\alpha^2)^{-1/2}v_{\mathbf{k}'}^2\gamma_{\mathbf{k}}/\gamma_0-u_{\mathbf{k}'}v_{\mathbf{k}'}\gamma_{\mathbf{k}-\mathbf{k}'}/\gamma_0\}+2u_{\mathbf{k}}v_{\mathbf{k}}\{(1-\alpha^2)^{-1/2}u_{\mathbf{k}'}v_{\mathbf{k}'}\gamma_{\mathbf{k}'}/\gamma_0-v_{\mathbf{k}'}^2\};$$

$$B_{\mathbf{kk}'}=(u_{\mathbf{k}}^2+v_{\mathbf{k}}^2)\{\tfrac{1}{2}(1-\alpha^2)^{-1/2}(u_{\mathbf{k}'}^2+v_{\mathbf{k}'}^2-\alpha)\gamma_{\mathbf{k}}/\gamma_0-u_{\mathbf{k}'}v_{\mathbf{k}'}\gamma_{\mathbf{k}-\mathbf{k}'}/\gamma_0\}+2u_{\mathbf{k}}v_{\mathbf{k}}\{(1-\alpha^2)^{-1/2}u_{\mathbf{k}'}v_{\mathbf{k}'}\gamma_{\mathbf{k}'}/\gamma_0-\tfrac{1}{2}(u_{\mathbf{k}}^2+v_{\mathbf{k}}^2)\}; \quad \text{(B2)}$$

$$C_{\mathbf{kk}'}=B_{\mathbf{kk}'}+\alpha(1-\alpha^2)^{-1/2}(u_{\mathbf{k}}^2+v_{\mathbf{k}}^2)\gamma_{\mathbf{k}}/\gamma_0.$$

If we apply a formula for second-order perturbation to (B1) and pick up a coefficient of $n_{\mathbf{k}\alpha}n_{\mathbf{k}'\alpha}$, $G_2$, defined by (45), becomes

$$G_2=-(2\gamma_0J/N^2S)\textstyle\sum_{\mathbf{k}''}(A_{\mathbf{kk}''}B_{\mathbf{kk}'}/f_{\mathbf{k}}+A_{\mathbf{k}'\mathbf{k}''}B_{\mathbf{k}'\mathbf{k}}/f_{\mathbf{k}'}+B_{\mathbf{k}''\mathbf{k}'}B_{\mathbf{k}''\mathbf{k}}/f_{\mathbf{k}''}), \quad \text{(B3)}$$

where an energy denominator of the perturbation formula, $\epsilon_{\mathbf{k}\alpha}^0+\epsilon_{\mathbf{k}\beta}^0$, is replaced by $4\gamma_0JSf_{\mathbf{k}}$, using (10). By substituting (B2) into (B3), we obtain (53) after some manipulations.

## APPENDIX C

The first two terms of (49) are written

$$-(2N)^{-1}\textstyle\sum_{\mathbf{q}}\{(X_{\mathrm{I}}/S_A-Y_{\mathrm{I}}/S_B)V_2(\mathrm{I})+(X_{\mathrm{VI}}/S_A-Y_{\mathrm{VI}}/S_B)V_2(\mathrm{VI})]$$
$$-\tfrac{1}{2}\sum\left\{\frac{[V_2(\mathrm{I})]^2}{\epsilon_{\mathbf{k}+\mathbf{q}\alpha}^0+\epsilon_{\mathbf{k}'-\mathbf{q}\alpha}^0-\epsilon_{\mathbf{k}\alpha}^0-\epsilon_{\mathbf{k}'\alpha}^0}+\frac{[V_2(\mathrm{VI})]^2}{\epsilon_{\mathbf{k}+\mathbf{q}\beta}^0+\epsilon_{\mathbf{k}'-\mathbf{q}\beta}^0+\epsilon_{\mathbf{k}\alpha}^0+\epsilon_{\mathbf{k}'\alpha}^0}\right\}, \quad \text{(C1)}$$

using (39) and (40).

We evaluate the first term of (C1) up to $k^2k'^2$, neglecting the terms with $k^2$ and $k'^2$ in $X_n$ and $Y_n$. Thus, using Table I, the first term of (C1) becomes

$$\cong-(8N\alpha S)^{-1}\textstyle\sum_{\mathbf{q}}(f_{\mathbf{k}+\mathbf{q}}f_{\mathbf{k}'-\mathbf{q}})^{-1/2}\{(1+f_{\mathbf{k}+\mathbf{q}})^{1/2}(1+f_{\mathbf{k}'-\mathbf{q}})^{1/2}-(1-f_{\mathbf{k}+\mathbf{q}})^{1/2}(1-f_{\mathbf{k}'-\mathbf{q}})^{1/2}\}\{V_2(\mathrm{I})+V_2(\mathrm{VI})\}. \quad \text{(C2)}$$

Here, for the sake of simplicity, we omitted a sign function, $\mathrm{sgn}\gamma_\kappa$, in the front of $(1-f_\kappa)^{1/2}$, because the final expression includes only square terms in $(1-f_\kappa)^{1/2}$. Using the expressions for $V_2(\mathrm{I})$ and $V_2(\mathrm{VI})$ given in Table II, we have

$$V_2(\mathrm{I})+V_2(\mathrm{VI})=(2J/N)/(1-\alpha^2)^{1/2}\textstyle\sum_{\delta}(\xi v_{\mathbf{k}}e_{\mathbf{k}}-\eta u_{\mathbf{k}})(\xi v_{\mathbf{k}'}e_{\mathbf{k}'}-\eta u_{\mathbf{k}'})(e_{-\mathbf{k}'+\mathbf{q}}+e_{-\mathbf{k}-\mathbf{q}})(u_{\mathbf{k}+\mathbf{q}}v_{\mathbf{k}'-\mathbf{q}}+v_{\mathbf{k}+\mathbf{q}}u_{\mathbf{k}'-\mathbf{q}}). \quad \text{(C3)}$$

Substituting (C3) into (C2), we write (C2) approximately as

$$-(J/8N^2)(1-\alpha^2)^{1/2}/\alpha^2S\textstyle\sum_{\mathbf{q}}[(1-f_{\mathbf{k}+\mathbf{q}}^2)/f_{\mathbf{k}+\mathbf{q}}+(1-f_{\mathbf{k}'-\mathbf{q}}^2)/f_{\mathbf{k}'-\mathbf{q}}]$$
$$\times\textstyle\sum_{\delta}\exp(i\mathbf{q}\cdot\boldsymbol{\delta})\{-2(\mathbf{k}\cdot\boldsymbol{\delta})(\mathbf{k}'\cdot\boldsymbol{\delta})+i(\mathbf{k}\cdot\boldsymbol{\delta})(\mathbf{k}'\cdot\boldsymbol{\delta})(\mathbf{k}'-\mathbf{k})\cdot\boldsymbol{\delta}-\tfrac{1}{2}(\mathbf{k}\cdot\boldsymbol{\delta})^2(\mathbf{k}'\cdot\boldsymbol{\delta})^2+2(ka)^2(k'a)^2/(\gamma_0\alpha)^2\}. \quad \text{(C4)}$$

After expansions of $f_{\mathbf{k}+\mathbf{q}}$ and $f_{\mathbf{k}'-\mathbf{q}}$ with respect to $\mathbf{k}$ and $\mathbf{k}'$, (C4) gives (56a).

In the second term of (C1), we have only to retain the primary terms in $V_2(\mathrm{I})$ and $V_2(\mathrm{VI})$ in the expansion with respect to $\mathbf{k}$ and $\mathbf{k}'$. They are

$$V_2(\mathrm{I})\sim V_2(\mathrm{VI})\cong JN^{-1}[(1-\alpha^2)/(\gamma_0\alpha^2)]\gamma_{\mathbf{q}}(\mathbf{k}\cdot\nabla)(\mathbf{k}'\cdot\nabla)\gamma_{\mathbf{q}}, \quad \text{(C5)}$$

where $\nabla$ is a gradient operator in $\mathbf{q}$ space. We easily obtain (56b) by substituting (C5) into the second term of (C1).

## APPENDIX D

The last term of (49) is written

$$-(\gamma_0JS)^{-1}\textstyle\sum_{\mathbf{q}}\tilde{V}_2(\mathrm{IV})V_2(\mathrm{IV})/(f_{\mathbf{k}+\mathbf{q}}+f_{\mathbf{k}'+\mathbf{q}}) \quad \text{(D1)}$$

in a long-wavelength approximation. A simple but troublesome treatment of (D1) gives the following primary term:

$$-\frac{J}{4N}\left(\frac{1}{\gamma_0S}\right)\frac{(1-\alpha^2)}{\alpha^2}(ka)^2(k'a)^2N^{-1}\sum_{\mathbf{q}}\left\{\frac{1}{f_{\mathbf{q}}^3}\left(\frac{8}{3}-2\frac{f_{\mathbf{q}}^2-\alpha^2}{\alpha^2}\right)\left(\frac{\gamma_{\mathbf{q}}}{\gamma_0}\right)^2-\left[\frac{4}{9}\frac{1}{f_{\mathbf{q}}^3}+\frac{10}{3}(1-\alpha^2)\frac{(\gamma_{\mathbf{q}}/\gamma_0)^2}{f_{\mathbf{q}}^5}\right]\frac{1}{\gamma_0a^2}(\nabla\gamma_{\mathbf{q}}\cdot\nabla\gamma_{\mathbf{q}})\right.$$
$$\left.+\frac{1}{9}\frac{1-\alpha^2}{f_{\mathbf{q}}^5}\left[1+5\frac{1-\alpha^2}{f_{\mathbf{q}}^2}\left(\frac{\gamma_{\mathbf{q}}}{\gamma_0}\right)^2\right]\frac{1}{\gamma_0^2a^4}(\nabla\gamma_{\mathbf{q}}\cdot\nabla\gamma_{\mathbf{q}})^2\right\}, \quad \text{(D2)}$$

where we used Table II and (41).